https://doi.org/10.5194/egusphere-2024-2244
Preprint. Discussion started: 30 September 2024


# Thermal State of Permafrost in the Central Andes (27°S-34°S)

Cassandra E.M. Koenig[1,2], Christin Hilbich[1], Christian Hauck[1], Lukas U. Arenson[3] & Pablo Wainstein[4]

[1]Department of Geosciences, University of Fribourg, Fribourg, Switzerland
[2]BGC Engineering Inc., Toronto, ON, Canada
[3]BGC Engineering Inc., Vancouver, BC, Canada
[4]BGC Engineering Inc., Calgary, AB, Canada

*Correspondence to*: Cassandra Koenig (cassandra.koenig@unifr.ch)

**Abstract**

The importance of monitoring the thermal state of permafrost has been widely acknowledged due to the numerous hazards associated with permafrost degradation under climate change. International collaborative efforts are in place to collate standardized permafrost monitoring data, with the goal of establishing baselines and early warning systems for potential consequences of large-scale permafrost loss. Most of these data have been compiled from circumpolar regions and mountain environments in the Northern Hemisphere, with a scarcity of ground temperature monitoring data in South America. To date, this lack of data has limited the understanding of the thermal state and possible degradation of mountain permafrost in Chile and Argentina. This study represents the first coordinated effort to compile and examine trends within ground temperature data from high altitude (i.e., 3,500 m to 5,500 m) mountain permafrost regions of the Central Andes. Ground temperature measurements were available from 53 boreholes installed by the private sector along a north-south transect at the Chilean-Argentine border (between 27°S and 34°S), within cold and warm permafrost, as well as in non-permafrost zones. The dataset reveals similarities in ground temperature characteristics with other mountain permafrost regions, including high spatial and temporal variability, correlations with altitude and slope aspect, and unique thermal attributes of rock glaciers. These observations suggest that the thermal regime of the Central Andes is shaped by processes similar to those of other mountain permafrost regions, a hypothesis previously proposed but not widely supported with data until now. With the longest record in the dataset spanning 9 years, it is currently not possible to determine whether ground temperatures are increasing in response to atmospheric warming. Instead, the high temporal variability observed in the data likely reflects short-term micro-climatic fluctuations and topo-climatic attributes unique to the Andean cryosphere - including hyper-arid conditions, intense solar radiation, lack of vegetative cover and organic matter, less massive ice (except for rock glaciers), and mountain topography in a southern hemisphere location. The susceptibility of the area to regional climatic phenomena (such as ENSO and PDO) implies that long-term trends may only be discernible from extended datasets spanning several decades. This highlights the need for continuous and ongoing monitoring of ground temperatures in the region. The study itself represents a unique and noteworthy collaboration between private industry, governments, and scientists, towards the advancement of understanding a key climate change indicator in a region with a paucity of ground-based data.

https://doi.org/10.5194/egusphere-2024-2244
Preprint. Discussion started: 30 September 2024


## 1 Introduction

Permafrost is an Essential Climate Variable (ECV) within the Global Climate Observing System (GCOS) and a cryospheric indicator of climate change (WMO, 2016; Streletskiy et al., 2017). Several studies have documented large-scale warming of permafrost in recent decades (e.g., Romanovsky et al., 2017; Derksen et al., 2019; Etzelmüller et al., 2020; Haberkorn et al., 2021; Nyland et al., 2021). Current research suggests that permafrost will continue to warm in many regions in the near term (i.e., 2031-2050) due to projected global increases in surface air temperatures, which could accelerate in the second half of the 21st century under extreme shared socioeconomic pathway (SSP) scenarios (Abram et al., 2019).

Near-surface (i.e., 0-10 m) thawing of permafrost is known to significantly impact land stability, causing subsidence and slope failures, and releasing water from ice-rich landforms in mountainous environments (Gruber and Haeberli, 2007; Krautblatter et al., 2010; Romanovsky et al., 2017; Kokelj et al., 2017). In Arctic and boreal regions, where permafrost soils store significant amounts of organic carbon (e.g. Schuur et al., 2009), permafrost thaw may amplify surface warming through the permafrost carbon-climate feedback (Schaefer et al., 2014; Koven et al., 2015; Schuur et al., 2015; Miner et al., 2022; Schuur et al., 2022). Understanding the present and potential future thermal conditions of permafrost is therefore essential for guiding the development of robust infrastructure and mitigating environmental risks in the face of climate change.

Two important parameters for characterizing and monitoring the thermal state of permafrost are 1) active layer thickness (ALT), or depth to permafrost; and 2) ground temperature measured at or below the depth of zero annual amplitude (DZAA). The active layer, classically defined as the layer above permafrost that freezes and thaws annually (van Everdingen, 1998), delineates the depth to the permafrost table when measured at the time of maximum annual thaw. This is distinct from the thermally defined active layer in permafrost regions, which is the distance from the ground surface to the DZAA and not necessarily associated with annual phase change (Dobiński, 2020). The DZAA represents the minimum depth at which seasonal temperature variations are fully attenuated by the ground and are no longer observable. It is often defined as the depth where seasonal amplitudes diminish to 0.1°C or less (van Everdingen, 1998). Ground temperature measured at or below the DZAA is therefore considered a good indicator of long-term permafrost thermal state because it represents the mean annual temperature of the ground over time (Lachenbruch and Marshall, 1986). Active layer thickness and temperature at the DZAA are both affected by changing climatic conditions, specifically rising air temperatures and changes to precipitation patterns that impact temporal snow distribution, which in turn strongly influences the transfer of heat from above the ground surface to depth (Isaksen et al., 2007; Christiansen et al., 2010; Biskaborn et al., 2019).

The importance of monitoring permafrost thermal state on a global scale has been widely recognized (Biskaborn et al., 2015; Smith et al., 2022), and international efforts have been established to gather standardized monitoring data of this kind. Most monitoring sites providing data to these programs are in polar and high mountain areas of North America and Europe, with fewer sites located in Russia, Central Asia, and Antarctica (e.g., Smith et al., 2022). Two examples of collaborative programs collecting permafrost temperature data are the Global Terrestrial Network for Permafrost (GTN-P) (Biskaborn et al., 2015) and the Swiss Permafrost Monitoring Network (PERMOS, 2019). In addition, ALT measurements have been collated as part

https://doi.org/10.5194/egusphere-2024-2244
Preprint. Discussion started: 30 September 2024


of the Circumpolar Active Layer Monitoring (CALM) network since the 1990s in the Arctic, Antarctic, and at many high elevation and mountain permafrost regions (Brown et al., 2000). Regional syntheses of these ground temperature and ALT data have provided documentation of permafrost thermal state at some locations for up to 40 years (e.g., Romanovsky, et al., 2010b), with many sites presenting evidence of increasing permafrost temperatures, particularly in the Arctic (Romanovsky et al., 2010a). Despite the progress towards a global synthesis of permafrost thermal state and trends with time, challenges remain in assessing linkages to long-term climatic change due to a general paucity of ground temperature monitoring boreholes, which are often sparsely distributed within permafrost regions and can have discontinuous records that are also limited in duration (Biskaborn et al., 2019; Smith et al., 2022). Common reasons for this include site access difficulties and high installation and maintenance costs. Unique objectives of individual instruments can also limit data collection coverage, especially in mountain permafrost regions (e.g., Noetzli et al., 2021).

The lack of ground temperature monitoring data, especially at depths greater than a few metres, is particularly pronounced in South America. Here, permafrost regions are largely understudied compared to other regions of the world (Arenson et al., 2022), despite an established awareness of the existence of permafrost in the Andes for many decades (e.g. ,Catalano, 1926; Corte 1953). Ground-based studies in this region tend to be scarce due to the high elevations, harsh climate, rugged terrain, and lack of infrastructure to access remote locations, which make data extremely challenging to obtain (Arenson and Jakob, 2010; Hilbich et al., 2022; Mathys et al., 2022). While some ground temperature monitoring studies in the Andes have been published (e.g., Trombotto et al., 1997; Trombotto and Borzotta, 2009; DGA, 2010; Andrés et al., 2011; Monnier and Kinnard, 2013; Atacama Ambiente, 2017; DGA, 2019; Nagy et al., 2019; Yoshikawa et al., 2020; Mena et al., 2021; Vivero et al., 2021; Table 1), most instruments have not been established for the explicit purpose of monitoring permafrost thermal change with time. Consequently, monitoring records in the region tend to lack the necessary duration and depth to discern average ground temperatures or warming/cooling trends below the DZAA, limiting comparisons of ground thermal state in the Andes with other regions where permafrost degradation is evident. For example, many ground temperature monitoring studies in South America have focused on estimating the lower regional altitude of permafrost and thus only collected temperature measurements up to depths of one metre and over periods of less than five years (Andrés et al., 2011; Nagy et al., 2019; Yoshikawa et al., 2020; Mena et al., 2021; Vivero et al., 2021). This lack of monitoring data from deep boreholes has been acknowledged to a certain degree in a proposed national monitoring plan for Chile (DGA, 2019), which includes recommendations for long-term monitoring of permafrost sites using boreholes ideally installed to the base of permafrost. However, installations under this plan have not exceeded 2 m in depth to date (Table 1).

On the other hand, some permafrost studies in the Andes have utilized deeper boreholes to characterize permafrost thermal conditions and to document changes in temperature over time. For example, Trombotto and Borzotta (2009) revealed permafrost degradation of a rock glacier in Argentina through a temperature monitoring record in a 5-m-deep borehole over a span of nearly 10 years, with an annual deepening of the active layer by up to 25 cm. Monnier and Kinnard (2013) reported the installation of two boreholes intended for ground temperature monitoring in the upper Choapa valley of northern Chile. These boreholes are equipped with thermistor strings reaching depths of 18 m and 25 m. Monitoring of the 25-m-deep borehole

https://doi.org/10.5194/egusphere-2024-2244
Preprint. Discussion started: 30 September 2024


between 2010 and 2013 has consistently shown stable temperatures close to the melting point of ground ice along the profile (i.e., 0°C), with an active layer estimated to range between 5-7 m deep (Monnier and Kinnard, 2013). In a third study by Atacama Ambiente (2017), approximately nine months of ground temperature measurements from three boreholes installed to depths ranging from 20-40 m at the Goldfields Salares Norte mining project in Chile were reported. The preliminary data from these boreholes indicated favorable conditions for the presence of permafrost between approximately 5 m and 13 m depth at one location, with the other two boreholes installed in unfrozen ground (Atacama Ambiente, 2017). While these six boreholes (only four of which are in permafrost) reported from three studies offer valuable insights into the thermal state and changes to permafrost, the fact that they represent the bulk of time-series measurements of ground temperatures in South America at depths greater than 2 m, emphasizes the absence of an Andes-wide data repository akin to what is available for the northern hemisphere. This lack of coordinated effort to compile continuous ground temperature monitoring data from sufficient depths hampers the development of a comparable understanding of permafrost dynamics across the region.

Despite the limitations highlighted in the preceding discussions, a unique opportunity currently exists to advance knowledge of permafrost thermal state in South America through collaboration between researchers and private industry. This is especially true in the border area of Chile and Argentina, which holds significant reserves of precious metals and other natural resources at different stages of exploration, extraction, and development. Site investigations that often include collection of ground temperature data in permafrost zones are necessary to support environmental permitting and engineering designs. Such monitoring generates valuable data that can be used to assess the ground thermal regime in regions which have yet to be documented and shared with the broader research community. In this study, subsurface thermal conditions along a North-South transect in the semi-arid Central Andes (27°S-34°S) were examined by summarizing ground temperature data from a suite of boreholes installed by the private sector at eight distinct industrial project sites (Figure 1). Temperature measurements presented herein were made available to the authors by BGC Engineering Inc., with the permission of the individual project owners. The data were accompanied by confidential field notes and reports containing relevant information regarding instrumentation and general site conditions during monitoring to support the interpretations presented in this study. All monitoring instrumentation was installed for environmental impact assessments (EIAs) or engineering design studies prior to the preparation of this paper.

https://doi.org/10.5194/egusphere-2024-2244
Preprint. Discussion started: 30 September 2024


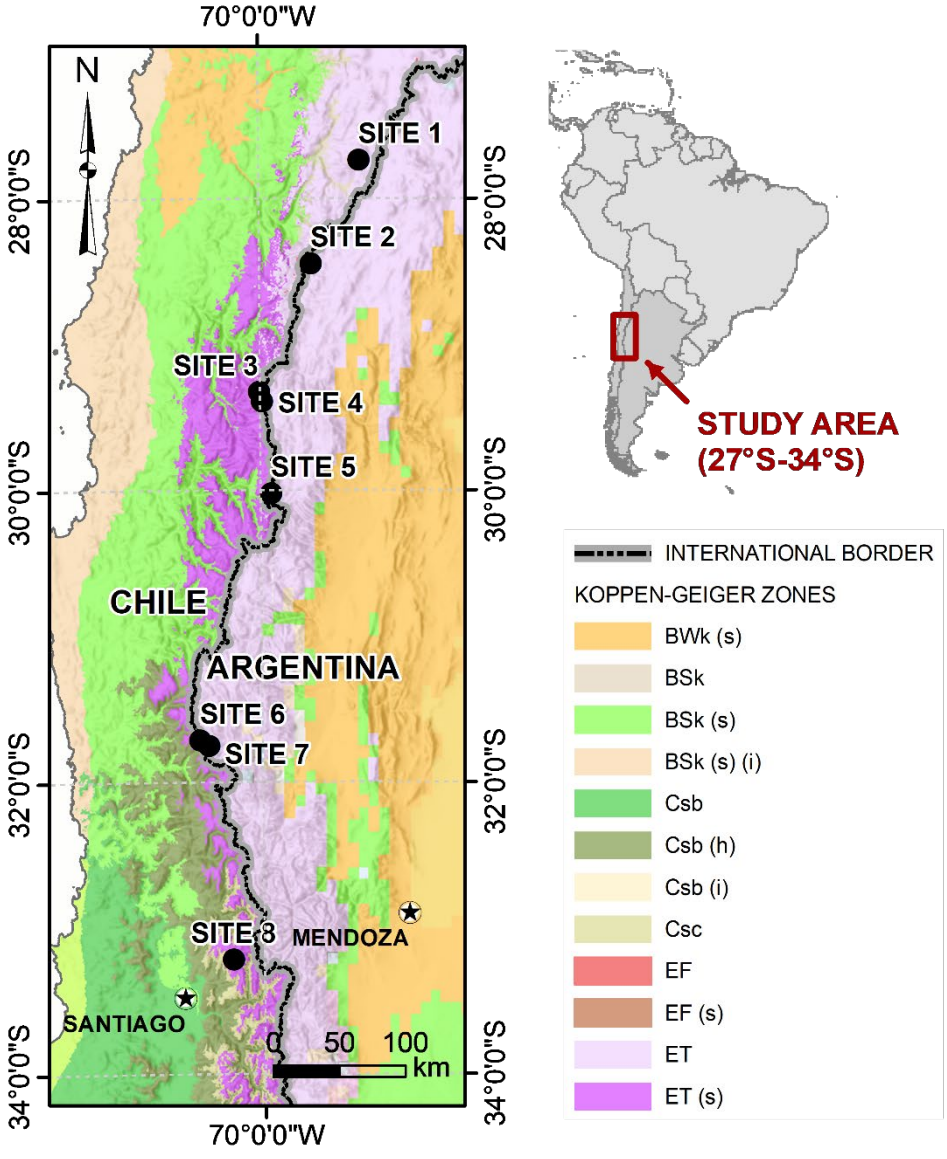


**Figure 1: Ground temperature monitoring locations and regional climatic setting.**

https://doi.org/10.5194/egusphere-2024-2244
Preprint. Discussion started: 30 September 2024


| Citation | Site Location | Approx. Lat / Long | No. Boreholes | Landform / Surface Substrate | Monitoring Location Name | Max. Measurement Depth (m) | Elevation (m) | Monitoring Record Length | Comments |
|---|---|---|---|---|---|---|---|---|---|
| Trombotto et al. (1997); Trombotto & Borzotta (2009) | Cordón del Plata range (Argentina) | 32°54'S-33°01S / 69°27'W-69°15W | 2 | Morenas Coloradas Rock Glacier | Balcón I | 5 | 3,560 | 1989-1992 + 5 manual measurements collected in summers of 2004-2008 | Inactive thermokarst (average temperature ~0°C; seasonal variation correlates with measured discharge; estimated deepening ~25 cm per year) |
| | | | | | Balcón II | 3 | 3,770 | 2001-2007 | Morenas Coloradas rock glacier, active thermokarst (permafrost deepening ~15 cm per year between 2002-2004) |
| DGA (2010) | Elqui River Catchment, La Laguna basin, Coquimbo (Chile) - Cerro Tapado, Topado | 30°06'S-33°24S / 69°59'W | 2 | Llano de las Liebres Rock Glacier | Liebres 1 | 2.7 | 4,050 | Apr-Dec 2010 | Permafrost (if present) is below deepest sensor and estimated to be at least 3m deep |
| | | | | | Liebres 2 | 7.4 | 3,786 | Apr-Dec 2010 | Permafrost (if present) is below deepest sensor and estimated to be at least 8m deep |
| DGA (2010); Vivero et al. (2021) | Elqui River Catchment, La Laguna basin, Coquimbo (Chile) - Cerro Tapado, Topado Complex | 30°06'S-33°24S / 69°59'W | 2 | del Topado Rock Glacier | BH1 (Tapado 1) | 2 | 4,440 | 2011-2015 | Permafrost (if present) is below deepest sensor and estimated to be at least 3m deep |
| | | | | | BH2 (Tapado 2) | 2.4 | 4,405 | 2011-2015 | Permafrost (if present) is below deepest sensor and estimated to be at least 2.6m deep |
| Andres et al. (2011) | Chachani volcanic complex (Peru) | 16°11S / 71°31'W | 3 | Slope of Chachani Volcano | CHACHA-1 | 1.2 | 4,850 | 2007-2008 | -- |
| | | | | | CHACHA-2 | 1.2 | 4,976 | 2007-2008 | -- |
| | | | | | CHACHA-3 | 1.2 | 5,331 | 2007-2008 | Possible permafrost location |
| Monnier & Kinnard (2013) | Andes Rock Glacier, upper Choapa valley (Chile) | 31°48S / 70°30'W | 2 | Quebrads Noroeste Rock Glacier | DDH2010-1 | 25.0 | 3,767 | 2010-2011 | 5–7m thick active layer |
| Centro de Estudios Avanzados en Zonas Áridas (CEAZA) | | | | | DDH2010-2 | 18.0 | ~3,800 | 2010-2011 | Measurements only performed 3 times per year |
| Atacama Ambiente (2017) | Goldfields Salares Norte Project (Chile) | 27°S / 68° W | 3 | -- | SNDD034 | 22.0 | 4,705 | Mar-Dec 2017 | Manual monthly measurements, non-permafrost borehole |
| | | | | | SNGET008 | 21.5 | 4,472 | Mar-Dec 2017 | Manual monthly measurements, non-permafrost borehole |
| | | | | | SNGET027 | 40.0 | 4,580 | Mar-Dec 2017 | Manual monthly measurements, permafrost from ~5-13 m deep |
| DGA (2019) | Tupungatito Volcano (Chile) | 33°S / 69° W | 2 | Rocky ridge, near Tupungatito glacier | Tupungatito A | 2.0 | 5,575 | 23-Dec-19 | -- |
| | | | | Rocky ridge, part of a lava flow from the Tupungatito volcano | Sitio B, Tupungatito | 1.2 | 4,425 | 24-Dec-19 | -- |
| | Glaciar Bello (Chile) | 33°S / 70°W | 1 | 100 m NW of Bello Glacier | Bello | 1.7 | 4,840 | -- | No measurements published in report |
| Nagy et al. (2019) | Mt. Ojos del Salado (Chile) | 26°56'S-27°29'S / 68°32'W-69°15'W | 6 | Debris Covered Plateau | Laguna Negro Francisco | 0.6 | 4,200 | 2014-2016 | -- |
| | | | | | Murray Lodge | 0.35 | 4,550 | 2014-2016 | -- |
| | | | | | Atacama Camp | 0.6 | 5,260 | 2012-2016 | Possible permafrost borehole |
| | | | | | Tejos Camp | 0.6 | 5,830 | 2012-2016 | Possible permafrost borehole |
| | | | | | Crater Edge | 0.2 | 6,750 | 2012-2016 | Possible permafrost borehole |
| | | | | | Mt. Ojos del Salado summit | 0.1 | 6,893 | 2012-2016 | Possible permafrost borehole |
| Yoshikawa et al. (2020) | Coropuna volcanic complex (Peru) | 15°32S / 72°32'W | 15 | Hydrothermally Altered Lava | Coropuna-N3 | 0.3 | 5,694 | 2012-2019 | -- |
| | | | | | Coropuna-N2 | 0.3 | 5,564 | 2012-2019 | -- |
| | | | | | Coropuna-S4 | 0.3 | 5,100 | 2012-2019 | -- |
| | | | | | Coropuna-S3 | 0.3 | 5,053 | 2012-2019 | -- |
| | | | | | Coropuna-N1 | 0.3 | 4,886 | 2012-2019 | -- |
| | | | | | Coropuna-S2 | 0.3 | 4,711 | 2012-2019 | -- |
| | | | | | Coropuna-S1 | 0.3 | 4,247 | 2012-2019 | -- |
| | | | | | Coropuna-Borehole | 3 | 5,170 | 2012-2019 | -- |
| | Chachani volcanic complex (Peru) | 16°13S / 71°29'W | | | CHACHANI-CH3 | 0.3 | 4,711 | 2012-2019 | -- |
| | | | | | CHACHANI-Borehole | 4 | 5,331 | 2012-2019 | Possible permafrost borehole |
| | | | | | CHACHANI-Borehole surface | 0.02 | 5,331 | 2012-2019 | Possible permafrost borehole |
| | | | | | CHACHANI-South facing | 1 | 5,329 | 2012-2019 | Possible permafrost borehole |
| | | | | | CHACHANI-Higher albedo | 1 | 5,323 | 2012-2019 | Possible permafrost borehole |
| | | | | | CHACHANI-CH2 | 0.3 | 4,700 | 2012-2019 | -- |
| | | | | | CHACHANI-CH1 | 0.3 | 4,200 | 2012-2019 | -- |
| Mena et al. (2021) | Chajnantor Volcano, Atacama (Chile) | 22°59S / 67°43'W | 1 | Slope of Chajnantor Volcano | -- | 14 | 5,640 | 2019 | Permafrost borehole, 5 m thick, gradient of 200°C/km; ALT ~ 14 cm |

**Table 1: Previously published ground temperature monitoring studies in permafrost regions of the Andes.**

https://doi.org/10.5194/egusphere-2024-2244
Preprint. Discussion started: 30 September 2024


## 2 Regional Setting

The study area is located in the Central Andes region (27°S-34°S), where the climate is strongly influenced by interactions between the southeast Pacific anticyclone (SEPA) and the Humboldt Current, as well as barrier effects of the mountainous terrain. Cold and humid westerlies associated with the Humboldt Current are diverted northward by the SEPA, while the Andean Mountain range deflects Pacific air masses upwards and limits the westward advection of moist air from the Amazon basin (Masiokas et al., 2020; Schulz et al., 2012). This results in the characteristic hyper-arid climate of the region and orographic precipitation that reaches its peak in the austral winter (June to August), falling predominantly as snow. Average annual precipitation across the region ranges between approximately 100 mm and 2,000 mm, with greater amounts generally observed at lower latitudes (Garreaud et al., 2020). The region also experiences pronounced climatic fluctuations on interannual and interdecadal timescales due to interactions between the El Niño Southern Oscillation (ENSO) and the Pacific Decadal Oscillation (PDO) (Mantua and Hare, 2002; Montecinos and Aceituno, 2003; Schulz et al., 2012; Vuille et al., 2015; Garreaud et al., 2020).

The eight project sites considered in this study are all situated at high altitudes, ranging in elevation from 3,500 m to over 5,500 m above sea level. Significant topographic variability also exists at the individual project level, with total relief ranging from 250 m to 1,200 m at any given site. As a whole, the study area falls within the 'Andean Arid Diagonal' (Bruniard, 1982), a contiguous zone of arid to semi-arid climate separating tropical and temperate climates of the northern and southern portions of the Andes (Figure 1). This includes portions of the Cold Mountain Desert (BWk) and High Mountain Tundra (ET) climatic belts (Kottek et al., 2006), which are distinguished by their unique variations in altitude, precipitation, and temperature trends. Climatic conditions of the BWk belt are dominant at elevations below ~4,000 m and are characterized by low humidity and minimal precipitation. Seasonal average temperatures range from ~18°C in January to ~8°C in July, making it highly unlikely for permafrost to exist or form in this zone. Instead, where permafrost does exist, it is expected to be naturally degrading. Rock glaciers are the most common periglacial landform within the BWk belt and have been shown to have variable ground ice contents across the study area, reflecting different degrees of permafrost degradation (Hilbich et al., 2022). In contrast, the climate of the ET belt (elevations generally >4,000 m) is associated with low temperatures year-round and mean annual air temperatures (MAATs) below 0°C (Vuille et al., 2003; Garreaud, 2009), creating favourable conditions for permafrost formation. Daily temperatures within the ET belt can exceed 15°C in summer months (December to February), but average temperatures typically remain below 10°C. Surface geomorphic indicators of permafrost have been identified in this belt both in the field and through remote sensed imaging, and include rock glaciers, gelifluction slopes, and in some cases, patterned ground (Arenson and Jakob, 2010). In both climatic belts, snow tends to accumulate at high altitudes during winter and remains frozen until spring (approximately October to November), following which a unimodal snowmelt-dominated regime is produced annually for all rivers originating from mountain peaks (Masiokas et al., 2016).

https://doi.org/10.5194/egusphere-2024-2244
Preprint. Discussion started: 30 September 2024


The distribution of permafrost across the Andes is complex, driven by high variability of mountain topography and climatic conditions at the catchment level. This variability leads to ground thermal conditions that can vary significantly over distances of tens to hundreds of metres. As with other mountain regions, slight variations in altitude (usually spanning a few hundred metres) can generate marked differences in air temperature, precipitation, vegetation, snowpack, solar radiation, and glacial cover over short lateral distances (e.g., Hock et al., 2019). However, the combination of hyper-arid conditions and intense solar radiation paired with a southern hemisphere location creates nuanced variations in water and energy balances, which uniquely shapes the distribution of permafrost in the Andes and distinguishes them from other mountain regions. The resultant effects on infiltration, subsurface freezing and thawing, and the movement of air and water through the ground contribute to the highly heterogeneous occurrence of permafrost in the region noted in several ground-based studies, with an even more complex distribution of ground ice (e.g., Hilbich et al., 2022). This tends to be particularly evident in rock glaciers, which have been shown to have considerable variations in ground ice content from case to case (Arenson and Jakob, 2010; Hauck et al., 2011; Mollaret et al., 2020; Halla et al., 2021; Hilbich et al., 2022) as well as within a single landform (Jones et al., 2019; Halla et al., 2021). In the southern Central Andes (32°S–36°S), the present-day lower altitudinal limit of permafrost has been estimated between 2,900 m and 3,200 m, with occasional occurrences up to approximately 3,700 m (Saito et al., 2016). This is known to vary with slope aspect due to variations in intensity of solar radiation, favouring the persistence of isolated patches of permafrost at lower elevations on pole-facing slopes compared to slopes oriented towards the equator (Yoshikawa et al., 2020; Arenson et al., 2022).

Several studies examining climate change in the region have identified a progression from a cooler humid climate to warmer and drier conditions in recent decades. A pronounced rise in air temperatures in the mid-1970s interrupted an existing period that was previously characterized by a slightly negative trend in maximum daily temperatures (Schulz et al., 2012). This air temperature rise was followed by a distinct downward trend in maximum and minimum air temperatures that continued into the early 2000s and coincided with a cold-to-warm sea surface temperature (SST) shift of the PDO to its cool phase (Schulz et al., 2012), which may have resulted in an increased frequency of El Niño events (Jacques-Coper and Garreaud, 2015). Between 1979 and 2006, Falvey and Garreaud (2009) observed a cooling of air temperatures on the order of 0.25°C/decade along the coast of Central and Northern Chile (from 17°S to 37°S). According to the authors, this was due to the emergence of cold water from the Humboldt Current promoted by southerly winds. For the same period, the authors report that inland meteorological stations (Lagunitas and Yeso) showed a steady warming of approximately 0.28°C/decade. Interactions of ENSO and IPO phenomena may have also contributed to a decline in precipitation during the last quarter of the 20$^{th}$ century (Schulz et al., 2012), as well as to the drought that currently persists in Central Chile (Garreaud et al., 2020). This sustained dry period (termed the “Central Chile Megadrought”) is the most extreme on record, with mean precipitation deficits up to 45% between 2010 and 2020 (Garreaud et al., 2020). Additionally, Carrasco et al., (2005) documented a regional elevation rise of the zero-degree mean annual air temperature (MAAT) isotherm in Central Chile from 1975-2001, with elevations rising by 122 m in winter and 200 m in summer. The increased energy availability associated with this shift facilitates snowmelt and a transition from solid to liquid precipitation, both of which could potentially trigger permafrost degradation in the area; as the

https://doi.org/10.5194/egusphere-2024-2244
Preprint. Discussion started: 30 September 2024


presence of snow cover modulates atmosphere-to-ground heat transfer (e.g., Zhang, 2005) and infiltration can enhance the absorption of latent heat, both factors impact the thermal regime of the ground.

## 3 Methodology

### 3.1 Monitoring Data and Permafrost Presence

Starting at various points in time between 2006 and 2017, ground temperature was systematically monitored at eight industrial project sites located between 27°S and 34°S and within approximately 25 km of the Chile-Argentine border (Figure 1). The compiled dataset includes measurements collected from 53 boreholes distributed across the region, with 27 located in Chile and 26 in Argentina. The boreholes were installed to depths varying from 10 to 100 m at surface elevations ranging from 3,625 m to 5,251 m. Ground temperatures were monitored along the profile of each borehole using Negative Temperature Coefficient (NTC) thermistor strings (models YSI 4400-, RST TH00-, or Geoprecision TNode-series). Sensors were positioned at varying depths reflective of the objectives of each borehole, starting from the ground surface (0 m) and at increasing spacings ranging from 0.5 to 15 m (depending on the maximum depth of the borehole). The frequency of data collection across locations is also variable, and ranges from hourly to daily measurements. Surface morphologies mapped at the boreholes at the time of thermistor installation can be broadly classified as bedrock, colluvium, rock glaciers (containing ground ice), and landslide deposits (Table S1). Except for instances where they are installed in rock glaciers, the boreholes typically intercept bedrock within ~10-20 m of the ground surface. Thus, measurements at most locations reflect thermal conditions of the deeper underlying bedrock.

The duration of monitoring varies across boreholes, ranging from less than one month to nine years, with several locations experiencing interruptions to data collection (Figure 2). These data gaps were attributed to numerous factors, including physical interferences (e.g., electrical storms), instrument malfunctions, and inaccessibility for data downloads or maintenance due to remoteness, adverse weather conditions, slope instability and/or changing regulatory requirements. In some cases, interruptions occurred simply because a borehole was temporarily not being monitored as part of the project's objectives. A comprehensive discussion of data collection challenges leading to monitoring gaps, along with known data artifacts and rationale for filtering is included in Section 3.2.

A continuous ground temperature monitoring record is required for a duration of at least two years to demonstrate the existence of permafrost (van Everdingen, 1998). Given the aforementioned data discontinuities and (in some cases) short monitoring duration, not all boreholes could be unambiguously designated as permafrost locations. For the purposes of this study, the criteria used for designating a borehole as a permafrost location required that monthly average temperatures remained at or below 0°C within the borehole for (1) at least two consecutive years with no measurement gaps, or (2) a longer period of time for instruments with data gaps, provided that at least one measurement was collected in each calendar month over the course of the entire record. Boreholes with temperatures below 0°C that did not meet these criteria were considered "possible permafrost" locations, and boreholes with temperatures above 0°C along the full profile were considered "non-permafrost"

https://doi.org/10.5194/egusphere-2024-2244
Preprint. Discussion started: 30 September 2024


locations (Figure 2). Permafrost and possible permafrost locations are referred to collectively in this paper as cryotic boreholes, and non-permafrost locations as non-cryotic boreholes. Gaps in individual monitoring records were filled according to the procedure outlined in Section 3.3 prior to further interpretations. The raw data for each borehole are presented within a series of plots compiled in the supplementary information package accompanying this paper (Figures S1-S53).

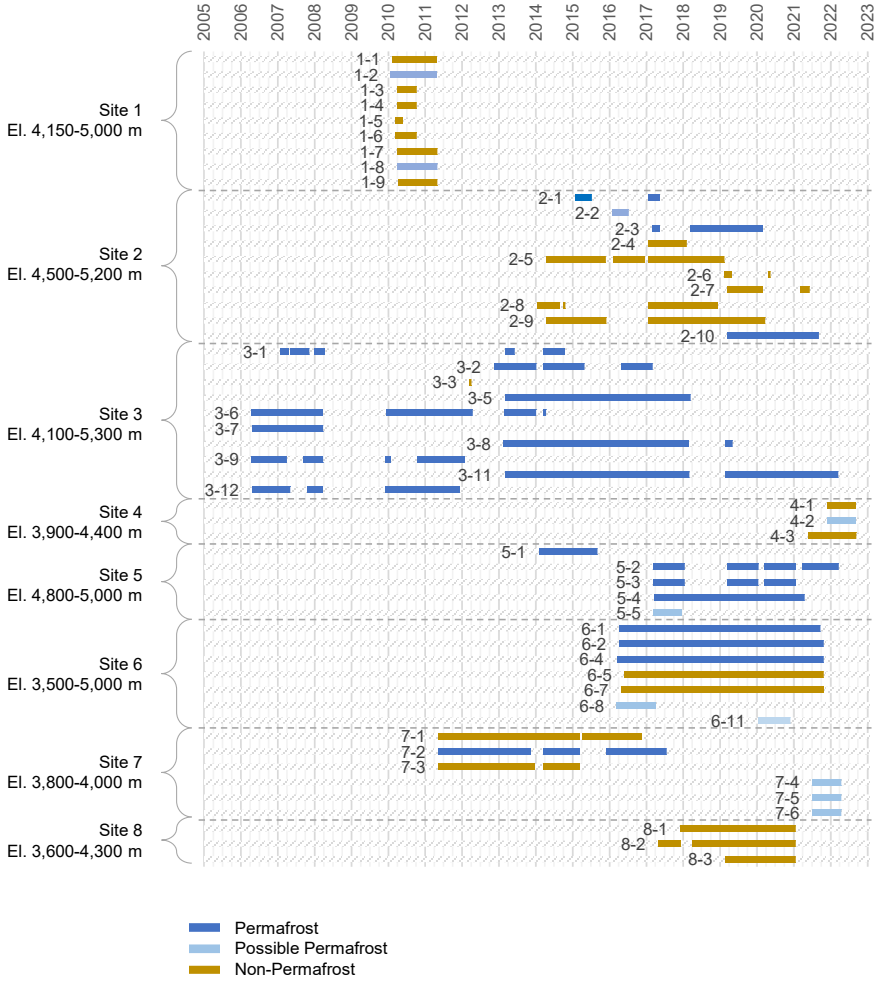


**Figure 2: Summary of available borehole temperature time series over time.**

### 3.2 Data Quality, Gaps and Filtering

The challenges with monitoring ground temperatures in high mountain regions are well documented in permafrost research (e.g., Noetzli et al., 2021). Long-term operation of borehole infrastructure in such environments can be hindered by natural

https://doi.org/10.5194/egusphere-2024-2244
Preprint. Discussion started: 30 September 2024


factors including erosion, mass movements or meteorological effects, all of which may lead to instrument malfunction that can reduce data quality or create gaps in monitoring records. Challenging logistics in blocky heterogeneous terrain, remoteness, as well as a lack of financial support can limit site access resulting in insufficient instrument maintenance and loss of data. Other impacts to ground temperature monitoring not necessarily limited to mountainous regions may result from instrument damage due to wildlife, vandalism, nearby construction activities or drilling and installation of the instruments themselves.

Many of these challenges were encountered across the monitoring sites in the current study, and documented instances of instrument interferences or malfunctions were used to identify and omit artifacts from the dataset prior to interpretation. In some cases, artifacts or recorded data errors were previously filtered by field staff and not stored in the dataset provided to the authors. From the available information, the most common reason for data interruptions stemmed from battery power loss, faulty connections, or sensor failures occurring between instrument maintenance visits. Since funding for ground temperature monitoring was not allocated to any of the projects on a regular basis (but instead depended on irregular work scopes and budgets that were driven by individual project objectives and regulatory requirements as they arose), predictability of field work was often lacking. Consequently, the instrument maintenance schedules were inconsistent and unpredictable, making it challenging to perform routine upkeep (such as replacing batteries or complete repairs on damaged sensors) proactively or in a timely manner over the various monitoring periods.

Drilling activities were also frequently identified as a source of interference to monitoring. While several thermistors were installed in pre-existing exploration boreholes, over half of the locations were drilled explicitly for ground temperature monitoring purposes. As such, early temperature measurements in these boreholes were potentially overestimated due to thermal disturbances from drilling. Locations affected included all boreholes at Sites 1, 4, 6 and 8, as well as boreholes 3-8, 3-11, 7-4, 7-5, 7-6 and 8-3. At Site 1, elevated temperatures are evident at the onset of monitoring, particularly from depths of 10 m and below (Figures S1-S9). Although temperatures gradually decrease as drilling-related disturbances dissipate, it remains uncertain whether ground temperatures at Site 1 had fully stabilized within the relatively short monitoring period of approximately one year. As they are unlikely to represent average ground temperature conditions, early measurements from Site 1 and other locations with approximately one year's worth of data (i.e., boreholes 6-8 and 6-11, 7-4, 7-5 and 7-6) were given less weight in the analyses conducted in this study, particularly those collected during the initial two to three months of monitoring. Drilling interferences were less of a concern for boreholes 3-8, 3-11, 8-3 and most boreholes at Site 6, which have longer monitoring records.

Changes in ground conditions were also understood to have potentially compromised the quality of measurements at several monitoring locations. For example, during a field visit in 2017, a sizeable gully was noted adjacent to borehole 5-1 that did not exist in previous years (Figure 3). Anomalies in the data and multiple sensor failures suggested that erosional activity associated with gully formation had affected borehole temperatures at this location since late 2015. Consequently, measurements beyond September 2015 were excluded from analysis. Another instance of natural ground disturbance influencing monitoring was noted during a 2017 field visit to borehole 2-2, where a previously unseen debris flow was observed

https://doi.org/10.5194/egusphere-2024-2244
Preprint. Discussion started: 30 September 2024


near the borehole (Figure 4). Similar to the situation at borehole 5-1, erroneous data were identified and excluded from analyses.

In some cases, project-driven optimization of monitoring also led to data interruptions (or shortened record lengths) and informed additional filtering. For example, data collection was discontinued at several boreholes at Site 2 once permafrost was determined to be absent, and thermistor strings were relocated to areas with a higher likelihood of encountering permafrost. This involved moving two thermistors (at boreholes 2-4 and 2-5) to higher elevations (boreholes 2-6 and 2-7), and thus termination of monitoring at the original locations. During the relocation of the thermistor originally deployed at borehole 2-4 to 2-6, it also became evident that the sensor at ~24 meters depth was damaged. Initially, anomalously high measurements recorded by this sensor at its original location were considered plausible, possibly due to warm groundwater or exothermic reactions at depth. However, similar anomalies persisted at the new location (borehole 2-6), suggesting measurements were artifacts and should be excluded from further analysis.

The supplementary information package accompanying this paper displays all raw data except for cases where artifacts were confidently identified and removed (e.g., related to erosion events or known instrument failures). Thermal disturbances from drilling and occasional unexplained artifacts are visible in the figures but were omitted from analyses. Unexplained anomalies could be the result of water or air flow through blocky materials, or common electrical storms which are common in central Chile (e.g., Montana et al., 2021). As there was no clear indication they were erroneous, these anomalies were retained on the plots for transparency and completeness of the dataset.

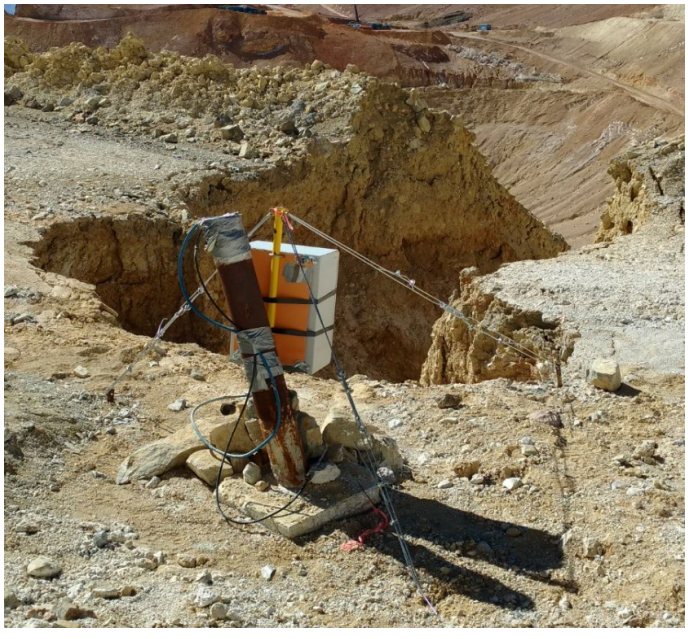

**Figure 3: Photograph of borehole 5-1 showing erosional gully that formed during the 2015 calendar year.**

https://doi.org/10.5194/egusphere-2024-2244
Preprint. Discussion started: 30 September 2024


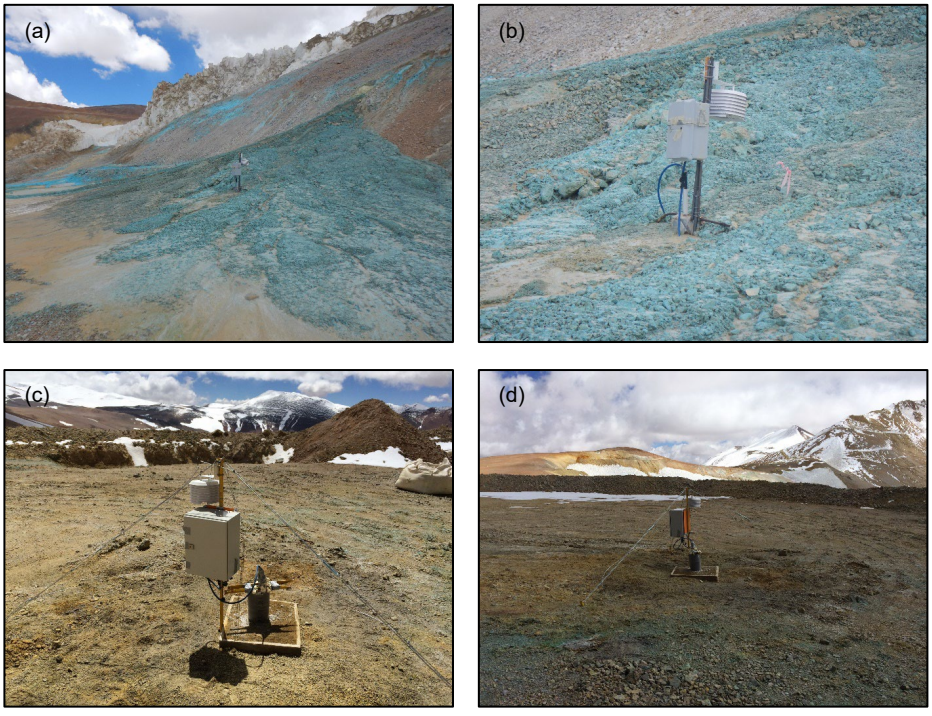


**Figure 4: (a) and (b) Original location of thermistor string at borehole 2-2 and the adjacent surface debris flows. The thermistor string was moved to boreholes 2-3 (illustrated in (c) and (d)) which is approximately 50 m higher in altitude.**

### 3.3 Filling of Data Gaps

Gaps in ground temperature time-series were interpolated using a non-linear least squares regression to enhance data visualization and remove seasonal bias from subsequent analyses. At thermistors that showed seasonal variation, a sinusoidal function with a superimposed linear trend was fit to filtered data to approximate seasonal and potential longer-term trends. For sensors located below the interpreted DZAA, a simple linear interpolation was used. Initial conditions for each sensor were specified by setting function parameters (i.e., period, amplitude, phase shift, offset, slope) that produced a reasonable visual match to observed data. Parameters were then optimized using the generalized reduced gradient (GRG) non-linear solver in Microsoft Excel to minimize the sum of squared residuals between observed and estimated values, with a target normalized root mean square (NRMS) value of less than 10%. The goodness of fit for each instrument was first assessed visually, and manual adjustments were occasionally made to improve the overall match of the solution to the data (NRMS values remained below 15%). Missing values in each thermistor record were then filled on a daily timestep using the fitted equation and are plotted together with raw data in the supplementary information package (Figures S1 through S53).

It is noted that this approach has limitations in estimating temperatures within the active layer or in boreholes containing ground ice due to its inability to represent latent heat effects during phase changes. Additionally, long records with complex

https://doi.org/10.5194/egusphere-2024-2244
Preprint. Discussion started: 30 September 2024


warming or cooling trends, which could also vary over the course of the monitoring period, cannot be represented using this approach. Despite these limitations, the method provided a useful way to estimate missing values and visualize seasonal patterns and general trends in the data and was considered reasonable for this study as the longest data record at a given instrument is less than 20 years.

## 4 Ground Thermal State

### 4.1 Seasonal and Interannual Ground Temperature Variations

A total of 22 cryotic (permafrost and/or possible permafrost) and 12 non-cryotic (non-permafrost) boreholes have continuous records spanning at least one year, making them suitable for examining seasonal effects on ground temperatures (Figure 5). Most instruments situated at depths near 10 m (Figure 5a) exhibit clear seasonal temperature fluctuations, with greater variation detected by sensors in unfrozen ground (amplitudes ranging from approximately 0.5°C to 1°C) compared to those within ground that remained below 0°C (amplitudes generally lower than 0.5°C). Sensors positioned at depths close to 20 m (Figure 5b), on the other hand, appear to be mostly below the DZAA, with a few exceptions in boreholes within non-cryotic ground. Within both the 10 and 20 m-depth suites of measurements, seasonal variations are less pronounced where ground temperatures hover around 0°C, reflecting latent heat effects associated with annual freezing and thawing of ground ice. Shallow ground temperatures (<2m) at a minimum of 14 monitoring locations exhibit dampened daily fluctuations during the winter, suggesting an influence of snow cover (Table S1). This is illustrated in the raw data time-series plots (Figures S1 through S53).

Unlike permafrost regions in the northern hemisphere, a consistent trend of rising ground temperatures over time is not discernable from the Andean dataset. Instead, individual monitoring locations appear to exhibit warming or cooling during their respective periods of record, with no correlation to location, altitude or surface substrate (Figure 5). A wide range in warming and cooling trends was noted for locations with at least two years of data (19 cryotic and 9 non-permafrost boreholes; Figure 6). Warming trends (ranging from 0 to 0.05°C /yr) were detected in approximately half of the boreholes examined (15), with the remaining locations showing cooling. Additionally non-cryotic boreholes appeared to exhibit greater variability in temperature change over time.

For comparison with other permafrost regions, Figure 6 includes representative warming trends documented in Smith et al. (2022) for continuous or “cold” Arctic permafrost (range: ~0.04 to 0.11 °C/yr and monitored since the 1980s), discontinuous or “warm” Arctic permafrost (range: ~0.01 to 0.05 /yr and monitored since the late 1970s to early 1980s) and mountain permafrost within the Swiss Alps (average: ~0.02 °C/yr and monitored since in the late 1980s to early 1990s). Interestingly, the estimated range in warming rates in the Andes align with those estimated for the Swiss Alps and the warm Arctic regions. Caution in this comparison is warranted however, as the northern hemisphere studies relied on significantly longer (decadal or multi-decadal) datasets than monitoring records in this study; the longest record considered in the Andean analysis was approximately nine years (borehole 3-11), with most records spanning between 2 and 7 years. In this context, the variability in the Andean dataset more likely reflects local topo-climatic conditions and short-term climate fluctuations in mountainous

https://doi.org/10.5194/egusphere-2024-2244
Preprint. Discussion started: 30 September 2024


terrain. To establish causal relationships between ground temperatures and longer-term climate variability to a similar level of confidence as has been accomplished for other permafrost regions, ongoing monitoring of ground temperatures alongside local climate variables is needed. Given the constraints of the current monitoring dataset, a comprehensive analysis of this scale is beyond the scope of this study and presents an opportunity for climate researchers.

https://doi.org/10.5194/egusphere-2024-2244
Preprint. Discussion started: 30 September 2024


**Figure 5: Monthly ground temperatures at depths of 10 m (a) and 20 m (b) at boreholes with at least a full year of measurements. Measurements in bedrock and in rock glaciers are plotted every two months for clarity in the figure.**

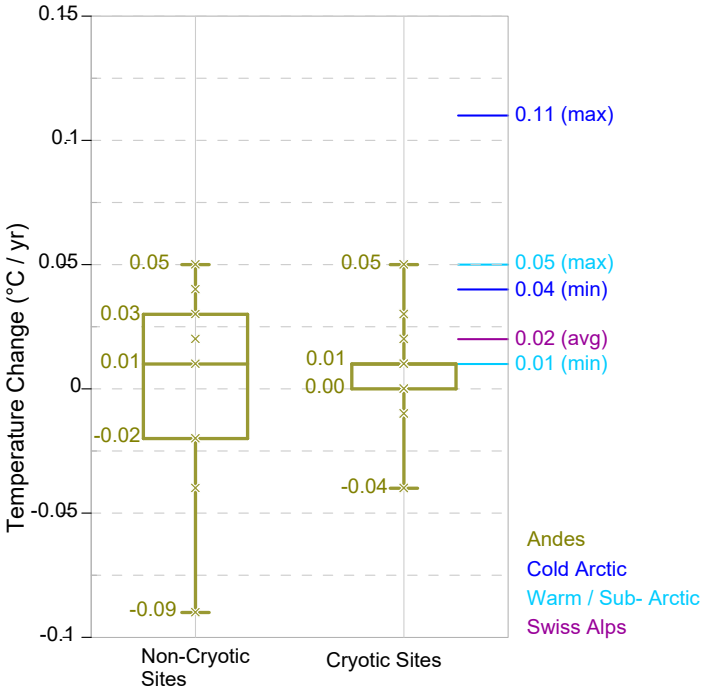


**Figure 6: Variation in ground temperature trends at 20 m depth in the Andes, and comparison with trends in permafrost regions in the northern hemisphere as reported by Smith et al., (2022). Note that rates for northern hemisphere studies were derived from decadal / multi-decadal datasets. Trends in the Andean dataset were estimated through interpolation of continuous measurements at locations where at least two years' worth of data was available. Trends are summarized in Table S1 with corresponding $r^2$ values.**

### 4.2 Depth to Permafrost

The thickness of the active layer (or ALT) in cryotic boreholes was estimated by linearly interpolating measurements between thermistors positioned above and below the zero-degree isotherm at the time of maximum annual thaw. Two permafrost locations (boreholes 3-7 and 3-12) were excluded from this exercise because the depth of thaw penetration remained above the shallowest sensors (i.e., < 1 m deep). Within two rock glaciers (boreholes 6-1, and 6-4), the depth to permafrost exceeded the maximum depth of annual freeze/thaw. Therefore, the measurement of interest at these locations is more appropriately termed depth to permafrost table as opposed to ALT. At locations where permafrost was possible but not confirmed due to insufficient length of monitoring, the maximum annual thaw depth was estimated in a similar manner to ALT (or permafrost table) for cases where the data record encompassed a complete freeze-thaw cycle with subsequent refreezing. This included two locations at Site 1 (boreholes 1-2 and 1-8). Possible permafrost locations with shorter monitoring records were not considered. This process was thus completed for a total of 20 boreholes using the filtered and gap-filled data (Sections 3.2 and 3.3).

https://doi.org/10.5194/egusphere-2024-2244
Preprint. Discussion started: 30 September 2024


Thaw depth and ALT typically range from ~0.5 to less than 4 m, although ALT at boreholes 3-5 and 6-2 reached depths ≥ 6 m (Figures 7 and 8). Notably, depth to permafrost within rock glaciers is the highest within the dataset, ranging between 7.3 to 17.4 m below the ground surface during the 2021 calendar year. This is consistent with surficial evidence of advanced degradation noted by the field staff for these specific landforms, although is not necessarily representative of conditions in rock glaciers across the region in general. Similar to the ground temperature time series, there does not appear to be an overall trend in deepening of the active layer over time across the dataset as might be anticipated with progressive atmospheric warming. In some locations, the active layer may even show signs of shallowing (e.g., boreholes 3-6 and 3-9, and possibly 2-10). Deepening of permafrost over time appears to be restricted to boreholes installed in rock glaciers, which are estimated to be lowering at rates of approximately 0.4 m/yr at borehole 6-1, 0.8 m/yr at borehole 6-2 and 1.5 m/yr at borehole 6-4. Contour diagrams of borehole temperature evolution with time (Figure 8) illustrate the presence of supra-permafrost taliks at boreholes 6-1 and 6-4. At borehole 6-4, the diagram shows that the top of permafrost was fully decoupled from the active layer throughout monitoring. In contrast, the formation of the talik at borehole 6-1 appeared to begin in mid-2019. Estimates of the maximum annual depth to permafrost across the site are included in Table S1 alongside the date for which the estimates were made.

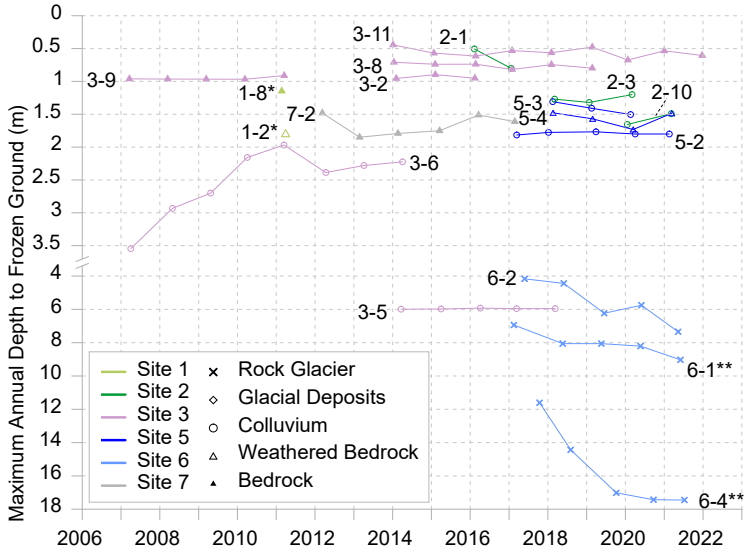


**Figure 7: Maximum annual depth to frozen ground within permafrost and possible permafrost boreholes. Note scale break between 3.5 and 4m. * indicates thaw depth (boreholes 1-2 and 1-8); ** indicates depth to permafrost table (boreholes 6-1 and 6-4). Active layer thickness (ALT) is plotted for all other boreholes. See text for additional detail.**

https://doi.org/10.5194/egusphere-2024-2244
Preprint. Discussion started: 30 September 2024


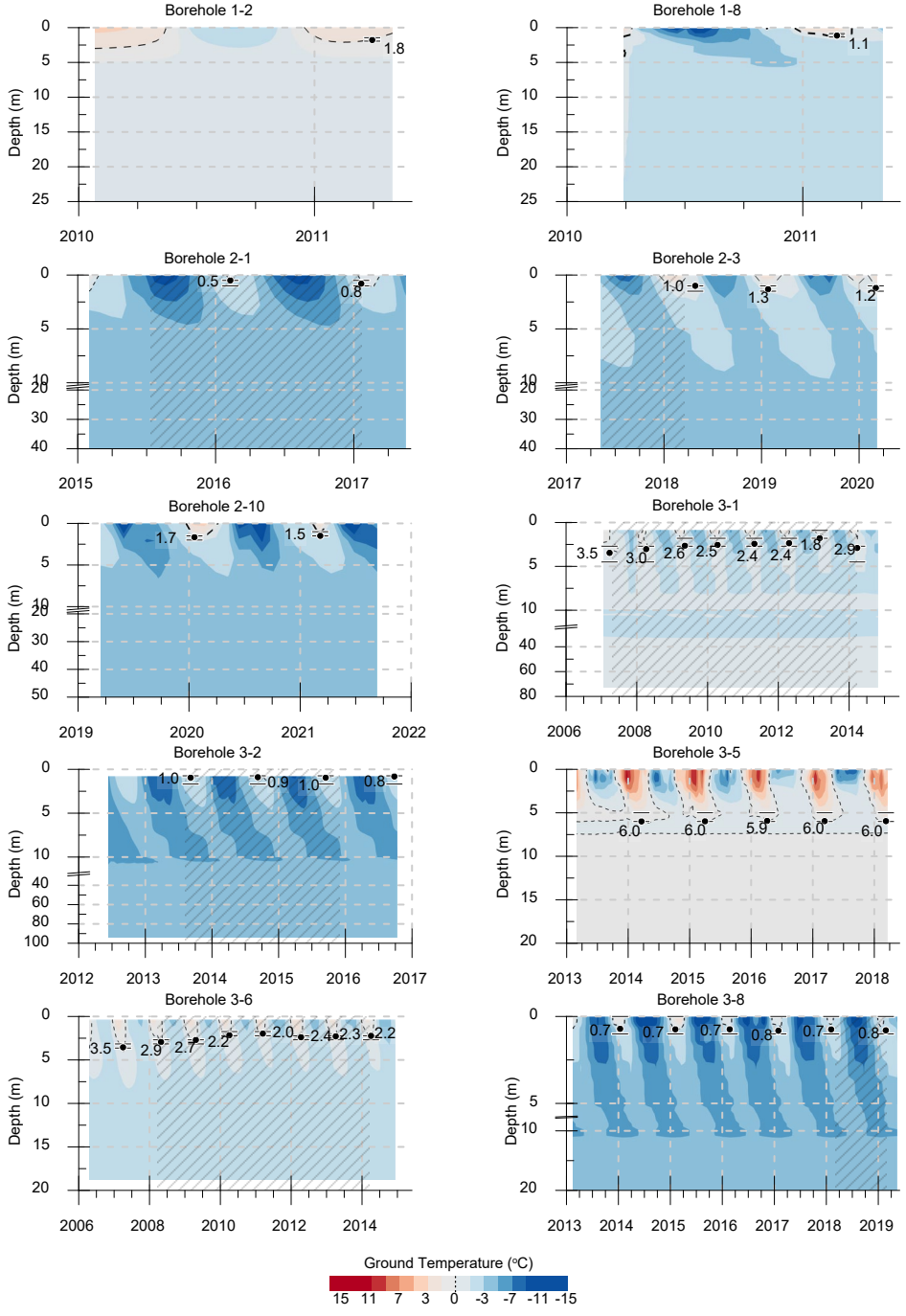


385 **Figure 8: Interpreted borehole temperature evolution with time. Ground temperature contours estimated from raw data and gap-filled values; data gaps filled by interpolation are indicated by grey hatched areas. Depth to permafrost is indicated by black dots; horizontal lines indicate the depth of thermistors used to estimate permafrost depth. Note breaks in y-axes at selected boreholes for improve contour visualization.**

https://doi.org/10.5194/egusphere-2024-2244
Preprint. Discussion started: 30 September 2024


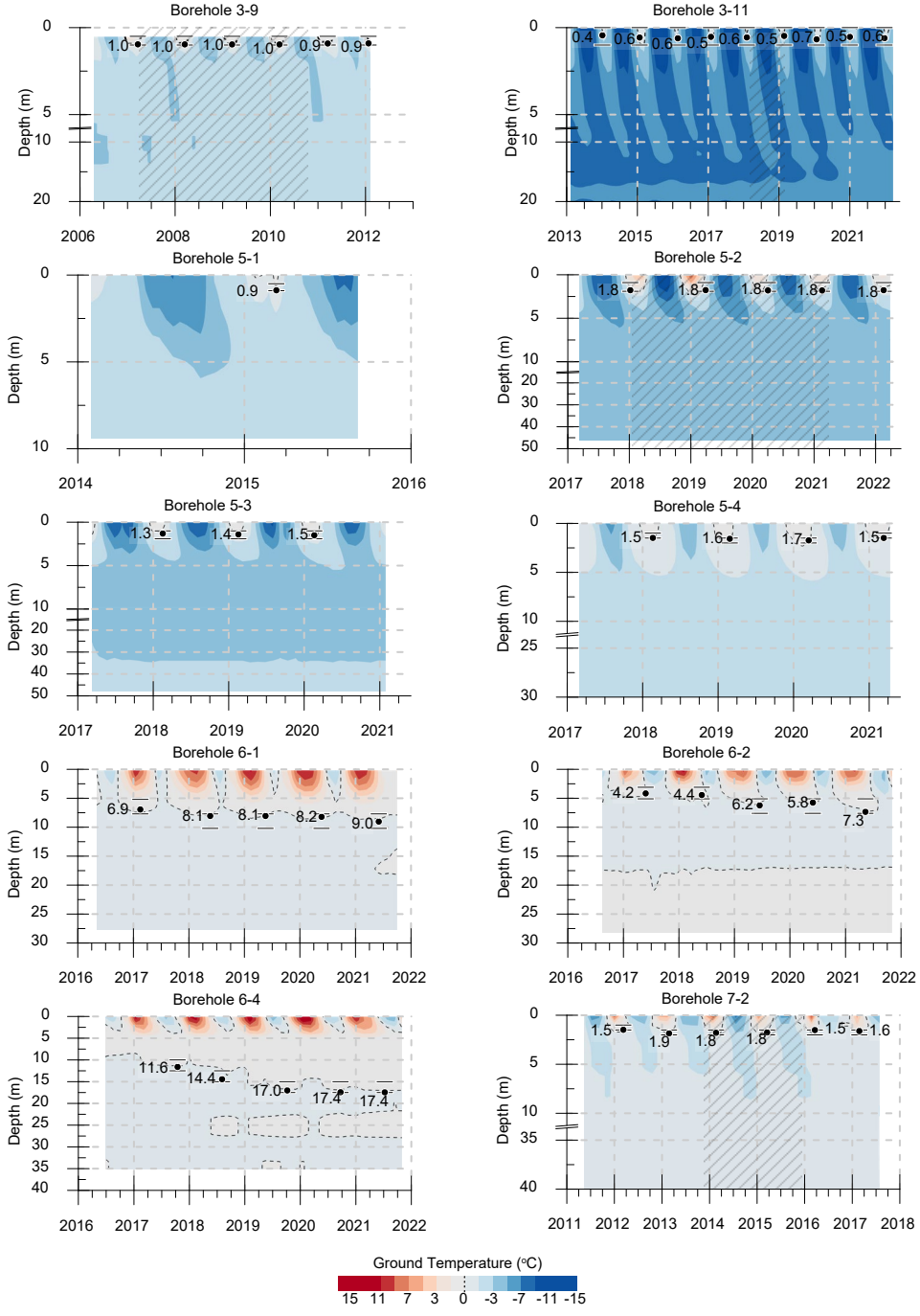


**Figure 8 (cont.): Interpreted borehole temperature evolution with time. Ground temperature contours estimated from raw data and gap-filled values; data gaps filled by interpolation are indicated by grey hatched areas. Depth to permafrost is indicated by black dots; horizontal lines indicate the depth of thermistors used to estimate permafrost depth. Note breaks in y-axes at selected boreholes for improve contour visualization.**

https://doi.org/10.5194/egusphere-2024-2244
Preprint. Discussion started: 30 September 2024


### 4.3 Ground Temperature Profiles

The temperature profile within a borehole may be affected by four primary factors: regional geothermal heat flux, depth-related lithology variations, local ground surface topo-climatic variations (which shapes the upper thermal boundary), and historical fluctuations in ground surface temperatures. These factors contribute to a variety of distinct profile shapes and broad range in ground temperatures across the dataset (from approximately -7 to 7°C, Figure 9), which reflect the complex thermal landscape of the Andes. The variability of profile shape within individual boreholes suggests that ground temperatures are generally not in equilibrium with modern climate conditions. Instead, they represent the present balance between surface and geothermal heat fluxes controlled by thermal properties of the ground, which vary across locations and uniquely along each borehole. Within the upper 30 m of measurements, thermal gradients were observed to be both positive (warming with depth) and negative (cooling with depth), while some locations exhibit roughly isothermal conditions. Several boreholes in warm permafrost (3-5, 6-2, 6-5, 6-8, 6-11, 8-3) exhibit a composite temperature profile within this depth range. These boreholes are characterized by a nearly isothermal region where temperatures are close to 0°C, below which temperatures increase with depth due to the heat flux from the natural geothermal gradient. The temperature profiles shown in Figures S1 through S53 reveal the presence of relatively thin layers of permafrost in several boreholes within rock glaciers, which vary in thickness from approximately 2 to 40 m. Within cryotic boreholes that did not intercept the base of permafrost (but exhibited warming with depth), permafrost thickness is estimated to range from 40 to > 500 m from projection of thermal gradients to the zero-degree depth intercept. Estimates of permafrost thickness are summarized in Table S1.

In general, there does not appear to be a relationship between profile gradient or curvature, or estimated permafrost thickness with latitude (i.e., site number) or surface morphology (Figure 9). This is not surprising given the wide range in ground surface elevations and surface slope orientations that occur within a few tens of metres at any given project site (Table S1 and Section 3.3). Topographic heterogeneity at this scale can lead to strong variations in surface solar radiation and microclimatic conditions that are likely to exhibit a greater influence on ground temperatures than variations in latitude would. While some variability in profile curvature may reflect contrasts in thermal properties of surface substrates, most boreholes are known to have intercepted bedrock below 10-20 m (BGC Engineering Inc, Pers. Comm. October 2023). Hence, it is reasonable to assume that most thermal gradients below the DZAA primarily reflect thermal properties of shallow bedrock with surface substrates exerting little to no influence on measurements.

Exceptions to this, however, arise in boreholes installed in rock glaciers, which contain varying amounts of ground ice and reach thicknesses up to approximately 40 m in this dataset. The coexistence of air and ice in the pore space near the ground surface and within the active layer of these coarse blocky landforms results in a significantly lower thermal conductivity of the medium compared to bedrock. In addition, the relatively large pore space promotes air convection, which can significantly cool the active layer, leading to temperatures ~1°C colder than without convection (e.g. Wicky and Hauck, 2020). Below the active layer, the ice-rock mixture is likely to be less sensitive to variations in the near-surface thermal regime (although still distinct from bedrock), leading to a unique profile shape despite possibly similar thermal histories at the ground surface.

https://doi.org/10.5194/egusphere-2024-2244
Preprint. Discussion started: 30 September 2024


Additionally, the evolution of ground temperatures over time would be notably influenced if there is appreciable ice content within rock glaciers, particularly if ice-rich permafrost is near its phase change temperature. In conjunction with profile shape, these characteristics may allow unique inferences to be made about the anticipated evolution of ground temperatures in response to varying surface temperatures. For example, permafrost in rock glaciers at Site 6 is generally isothermal with depth at ~ 0°C, possibly because ground ice is melting. In contrast, the colder permafrost in rock glaciers at Site 7 (at approximately -1°C at 10 metres depth) exhibits a positive thermal gradient (warming with depth). Ground temperatures (and therefore profile shapes) within rock glaciers at Site 7 are likely to be more sensitive indicators of surface temperature change compared to Site 6, where potential temperature trends are obscured due to latent heat effects.

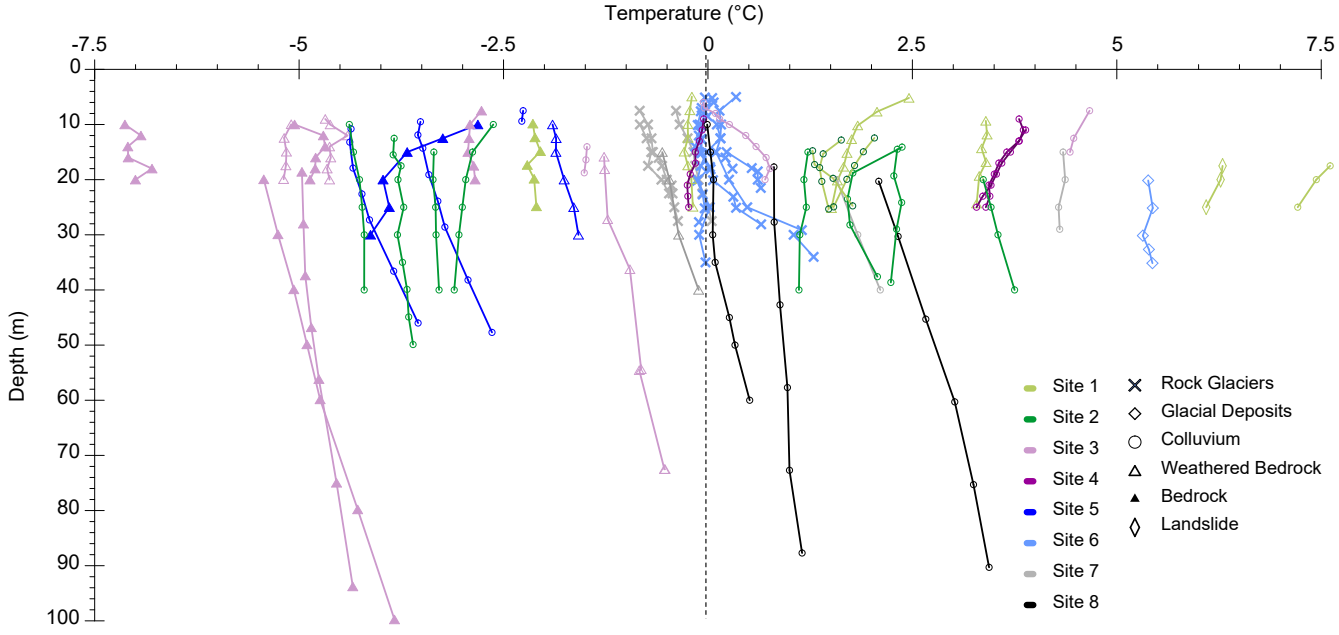


**Figure 9: Ground temperature profiles at all boreholes. Average and most recent values shown for locations with ≥1 year and <1 year of data, respectively. Excludes shallow measurements (between ~5-20 m) influenced by seasonal temperature variations.**

### 4.4 Thermal Gradients

While the assessment of warming or cooling trends presented in Section 4.1 is hindered by record length, the thermal gradients of individual boreholes may provide some insight into the recent thermal evolution of the ground in response to changing surface temperatures. Since temperature anomalies at the ground surface are attenuated by the subsurface, historical shifts in surface temperatures may be indicated by warm (or cool) side deviations observed in shallow temperatures from the linear trajectory of the deep gradient within a borehole. This temperature deviation (or offset) was estimated as the difference between projected surface temperatures from shallow (< 30 m) and deep (30-100 m) gradients. Offsets estimated from data collected in this depth range reflect recent decade-scale shifts in surface temperatures, assuming equilibrium conditions and uniform

https://doi.org/10.5194/egusphere-2024-2244
Preprint. Discussion started: 30 September 2024


thermal properties of the borehole with depth (e.g., Lachenbruch and Marshall, 1986). Since the time lag of thermal responses to warming of the ground surface at depths greater than ~100 m is likely to be several decades, the offset provides a first approximation of secular trends.

A total of 19 boreholes (10 cryotic and 9 non-cryotic boreholes) in the Andean dataset extend to depths greater than 30 m and were considered in this analysis. Rock glaciers were excluded due to their unique thermal profiles, as were measurements from boreholes 2-4 and 2-6 due to erroneous measurements at ~24 m (Section 3.2). Thermal gradients were estimated using measurements from the linear segments of profiles at intermediate depths (i.e., below the DZAA and up to approximately 30 m below the ground surface) and from 30 m to the final depth of each borehole, with one exception at borehole 8-1. The shallower gradient at borehole 8-1 was estimated from the DZAA to 60 m, and the deep gradient from 60 m onward due to a slight decline observed in the thermal gradient at approximately this depth (Figure 9). Results of the gradient analysis (Figure 10) are presented in a similar manner as the temperature trends derived from the interpolation of time-series data (Figure 6) for conceptual comparison of the two analyses. As with the time-series interpolation, the gradient analysis indicates both warming and cooling in recent history, with greater variability in the non-cryotic boreholes. Warm-side deviations from deep thermal gradients are evident for 14 of the boreholes (7 cryotic and 7 non-cryotic), and range from 0.05 to 0.9°C. The remaining boreholes (2 cryotic and 3 non-cryotic) indicate cooling in recent decades, with offsets ranging from approximately -0.05 to -1.08°C. It must be emphasized however that these estimates are derived from many simplifying assumptions, and that three-dimensional analysis of the geothermal fields, accounting for ground thermal properties, would be necessary for a more precise understanding of near-surface ground temperature changes in recent history.

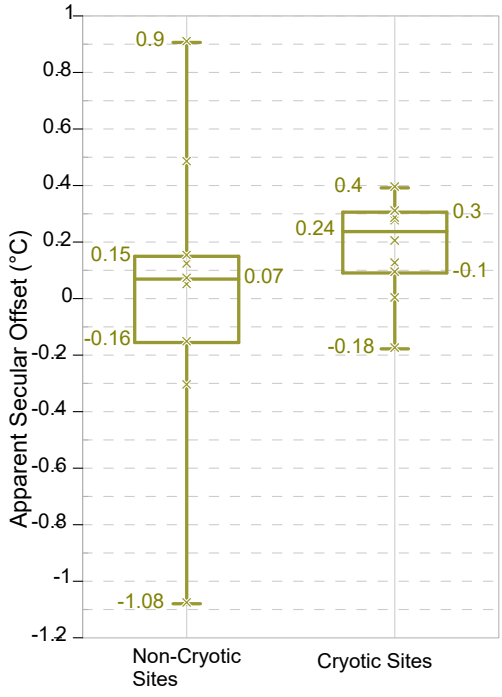

https://doi.org/10.5194/egusphere-2024-2244
Preprint. Discussion started: 30 September 2024


**Figure 10: Variation in apparent secular offset in ground surface temperatures, estimated from gradient analysis.**

### 4.5 Aggregate Trends

An examination of representative ground temperatures across the entire study region reveals no correlation between ground temperature and latitude; however, significant variation over short lateral distances is evident at the site level (Figure 11). This includes transitions from cold to warm permafrost (< -2°C to 0°C) and/or to non-cryotic ground over horizontal distances as small as 1 km in some cases, reflecting a greater influence of catchment-scale topo-climatic variability compared to regional climate variations. An overall lowering of ground temperatures across the dataset is observed as altitude increases, with generally no relationship to mapped surface morphology since most measurements represent thermal conditions of shallow bedrock (Figure 12a). Rock glaciers are again exceptions, with consistently lower average temperatures than boreholes at similar elevations (i.e., temperatures within rock glaciers are typically $\leq$ 0 °C, whereas other boreholes at similar elevations vary from approximately 2-6°C). Boreholes within rock glaciers also appear to mark the lowest altitudinal occurrence of permafrost within the dataset (slightly below 3,600 m) likely reflecting a sustained presence of ground ice due to latent heat combined with cooling effects of air convection within the blocky active layer compared to other surface substrates. With rock glaciers excluded, there is a slightly tighter correlation between ground temperatures and altitude at cryotic boreholes ($r^2 = 0.65$) than for the complete dataset ($r^2 = 0.53$), with lapse rates of approximately -4.3°C/km and -5.7°C/km, respectively. Consistent with an overall tendency towards cooler temperatures at higher altitudes, estimated depths to permafrost and permafrost thickness both decrease with increasing ground elevation (Figure 12b and c). Again, no correlation with surface morphology is evident in the dataset except for rock glaciers, which diverge from the general trend observed in the remainder of the boreholes (i.e., most variable depth to permafrost and lowest estimated thickness within the dataset). This departure reflects the unique constitution of the active layer in rock glaciers (elevated porosity and ground-ice) compared to the broader dataset, as well as the advanced state of degradation in these landforms (e.g., supra-permafrost talik formation at boreholes 6-1 and 6-4, Figure 8). Excluding rock glaciers, the relationship between permafrost depth and altitude is approximately -1.9 m/km elevation gain ($r^2 = 0.30$). Permafrost thickness appears to increase with increasing altitude at approximately 300 m/km ($r^2 = 0.45$).

Incorporating slope aspect into the analysis reveals that the zero-degree isotherm for ground temperature occurs at higher elevations on the north-east facing slopes, ranging from below 3,700 m (within rock glaciers) to approximately 5,000 m (Figure 13a). This asymmetry may be attributed in part to variations in average incident solar radiation with aspect (Figure 13b), and more broadly to the geographical position of the study area within the southern hemisphere. Coincidentally, all monitoring locations within rock glaciers are on south-facing slopes and in areas that experience lower solar radiation. In addition to their unique morphological characteristics, porosity and ground ice content, this lower average solar radiation may contribute to the persistence of permafrost in these particular landforms.

https://doi.org/10.5194/egusphere-2024-2244
Preprint. Discussion started: 30 September 2024


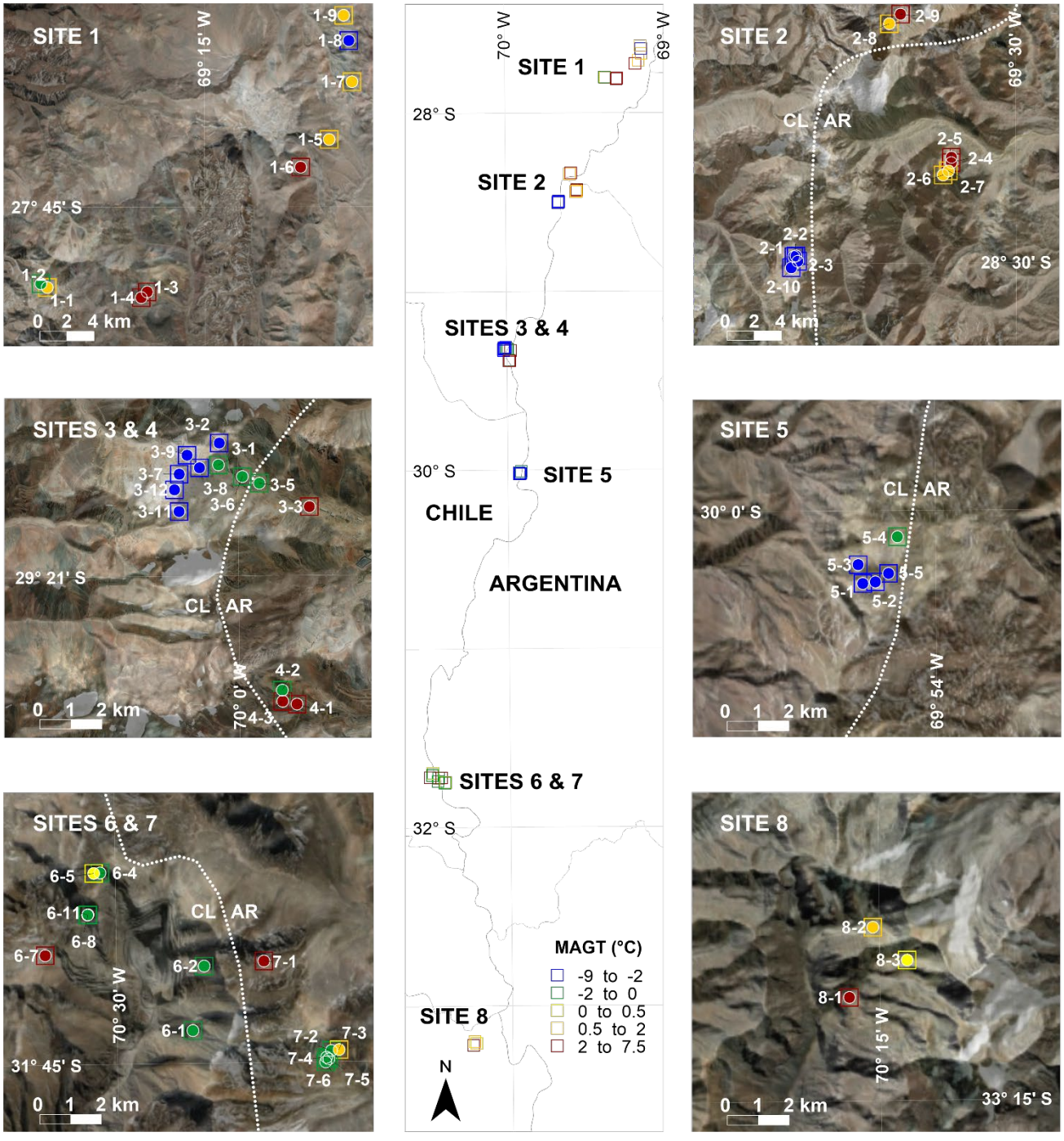


**Figure 11: Representative ground temperatures across the study area. Measurements are shown for depths of 20 m and/or within cryotic zones of the boreholes (boreholes 3-5, 6-2, 6-4, 6-8 and 6-11), or from the deepest sensor if the thermistor string was shorter than 20 m (boreholes 3-3 and 5-1). Temperature values and measurement depths are summarized in Table S1.**

https://doi.org/10.5194/egusphere-2024-2244
Preprint. Discussion started: 30 September 2024


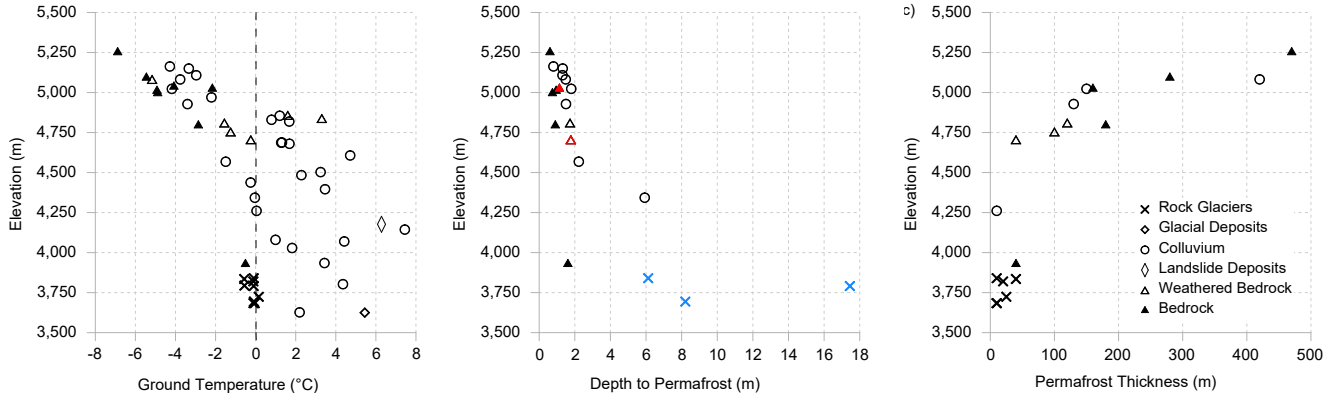


**Figure 12: Relationship of (a) ground temperatures and (b) depth to permafrost and (c) permafrost thickness with altitude. Thaw depth and depth to permafrost table coloured red and blue on diagram (b). The remaining points on diagram (b) represent the thickness of the active layer (ALT).**

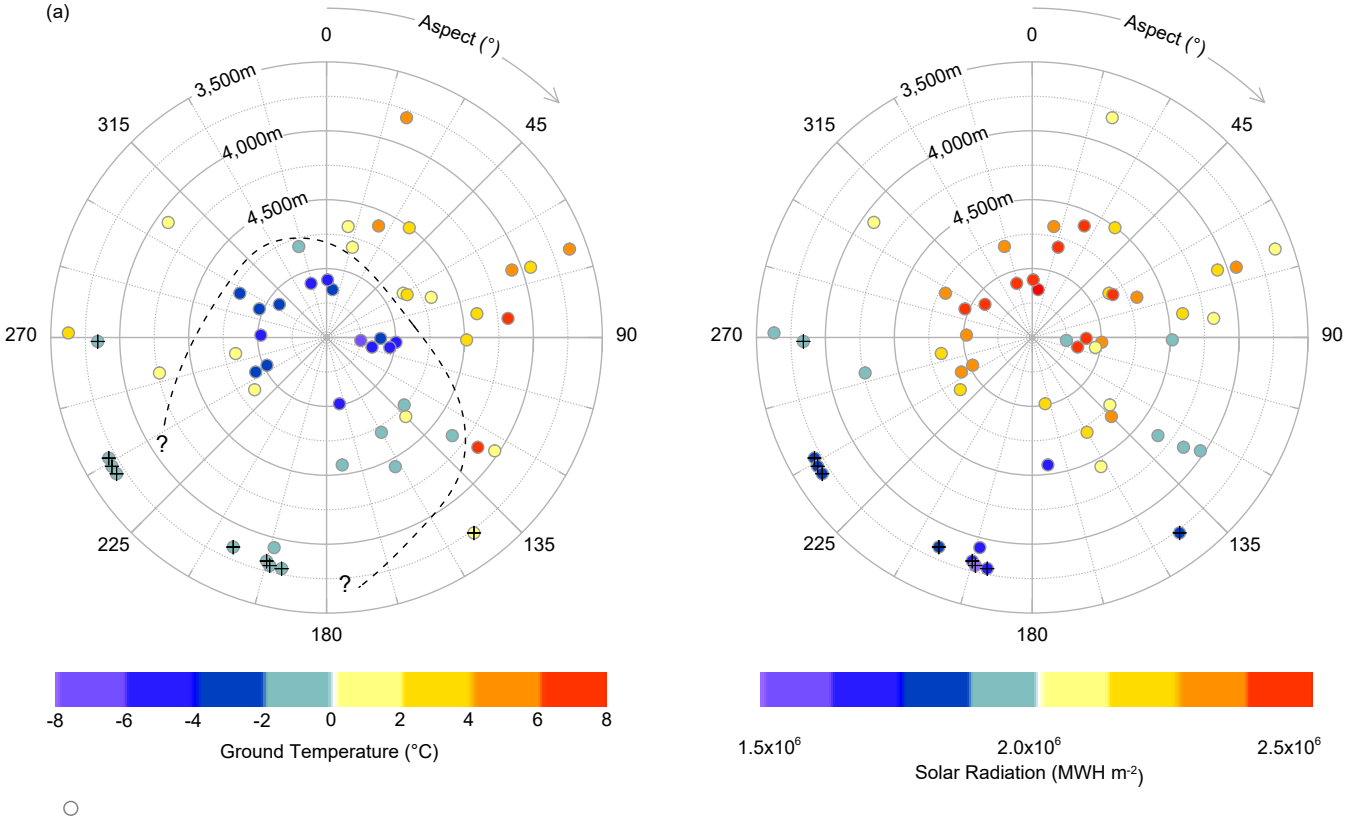


**Figure 13: Aspect-elevation diagrams showing variations in (a) ground temperature and (b) average incident solar radiation. Aspect was estimated from ASTER GDEM v3 Worldwide Elevation Data (1 arc-second Resolution). Solar radiation estimated using esri Area Solar Radiation toolset. (https://desktop.arcgis.com/en/arcmap/latest/tools/spatial-analyst-toolbox/area-solar-radiation.htm).**

https://doi.org/10.5194/egusphere-2024-2244
Preprint. Discussion started: 30 September 2024


## 5 Discussion

### 5.1 Significance of the Dataset

Permafrost extent, thermal state, and the nuanced thermal characteristics of rock glaciers have been well characterized through extensive research conducted in circumpolar regions and mountain environments of the northern hemisphere. Many studies have been able to unequivocally demonstrate permafrost degradation in response to atmospheric warming, as they are based on multi-decadal ground temperature datasets, some with measurement records spanning up to 40 years in length (e.g., Smith et al., 2022; PERMOS, 2023). Despite the growing interest and important strides towards building an understanding of permafrost in the Andes (e.g., Trombotto et al., 1997; Trombotto and Borzotta, 2009; DGA, 2010; Andrés et al., 2011; Monnier and Kinnard, 2013; Nagy et al., 2019; Yoshikawa et al., 2020; Mena et al., 2021; Vivero et al., 2021), the volume of research in the region remains comparatively limited. As a result, the understanding of permafrost in the Andes is less comprehensive than the well-established knowledge of permafrost elsewhere, highlighting the need to verify hypotheses using in-situ measurements. This study has revealed new insights into permafrost dynamics in the Central Andes, some which were previously hypothesized based on studies from other permafrost regions but lacked sufficient data to confirm their broader relevance to South America.

The present study constitutes the largest and most regionally extensive compilation of ground temperature data from high altitude (>3,500 m) sites with permafrost in South America to date. Using data from 53 boreholes varying from 10 m to 100 m in depth and within both permafrost and non-permafrost zones, the compilation provides a unique snapshot of ground thermal state within the Andean Cordillera of Chile and Argentina. Adequate depth of monitoring throughout the dataset allows for a depiction of average temperatures below the depth of seasonal influences, visualization of borehole thermal gradients, and first-order estimates of the thickness of, and depth to, permafrost. This level of insight surpasses that of the few key existing monitoring studies in the Andes, which typically are limited to boreholes that reach only a few meters in depth (Trombotto et al., 1997; Trombotto and Borzotta, 2009; DGA, 2010; Andrés et al., 2011; DGA, 2019; Nagy et al., 2019; Yoshikawa et al., 2020; Mena et al., 2021; Vivero et al., 2021).

Perhaps the most important implication of this work is that the data can be used to substantiate existing characterizations of permafrost distribution in the region, which were previously developed from field observations and statistical methods, but without borehole temperature data (e.g., Arenson and Jakob, 2010; Ruiz and Trombotto, 2012). Additionally, the availability of ground temperature data within permafrost and non-permafrost zones in this study reduces the risk of site-selection bias towards permafrost presence, which can complicate evaluations of spatially distributed models predicting permafrost. Beyond validating existing permafrost distribution models in the region, data from this study may also be utilized to support upscaling endeavors like those of Mathys et al. (2022), which aim to quantify ice content in Andean permafrost regions and provide crucial insights for future water resource planning and decision-making amidst the challenges posed by climate change.

On its own, several important insights can be derived from the presented dataset that broaden the understanding of permafrost thermal state in both the Andes and the global permafrost context. Some of these insights are consistent with observations in

https://doi.org/10.5194/egusphere-2024-2244
Preprint. Discussion started: 30 September 2024


other permafrost regions, while others could be uniquely representative of the Central Andes, or more precisely, within the altitudinal and latitudinal constraints of the dataset (i.e., 3,625 m to 5,251 m and 27°S-34°S). These are discussed in the sections that follow.

### 5.2 Ground Temperature Evolution and Response to Climatic Influences

A distinguishing characteristic of the presented dataset from other permafrost studies is that the Andean data do not show a clear indication of warming in recent history; rather, they indicate both warming and cooling over time, seemingly without correlation to location, elevation, or surface substrate. This is observed in the time series data (Section 4.1) and deduced from analyses of thermal gradients (Section 4.4), with the lack of correlation between temperature change with topography for both methods illustrated (Figure 14a and Figure 14b). Both analysis methods present limitations to data interpretation, notably the short record length in time series (<10 years) hindering the assessment of long-term trends, and the analyses of thermal gradients (despite potentially being more reliable indicators of decadal-scale temperature change) relying on numerous simplifying assumptions about the medium. Some variability in temperature evolution with time may, however, reflect local topographic conditions and short-term climate fluctuations that obscure longer-term global trends. Similar short-term permafrost temperature fluctuations, which deviate from long-term air temperature rises and are linked to local meteorological conditions, are known to exist within global datasets despite overarching trends of subsurface warming (Biskaborn et al., 2019; Etzelmüller et al., 2020; Haberkorn et al., 2021). Additionally, localized changes in snow cover, vegetation, and soil moisture content, especially in mountain environments, are known to significantly impact the thermal state of the ground. For example, periods of permafrost cooling in the Alps were observed during 2016 and 2023 and attributed to anomalously low snow conditions (PERMOS, 2023). Also in the Alps, summer heat waves during 2016 and 2019 were shown to correlate with short-term increases in active layer thickness (PERMOS, 2023), and water percolation has been shown to accelerate permafrost degradation (Luethi et al., 2017). At several of our monitoring locations in the Andes, snow cover variability may be inferred by the occurrence of near-surface isothermal conditions within the active layer from year to year (Figures S1 through S53). This would contribute to both the temporal and spatial variability in ground temperatures observed in the presented dataset due to irregular insulation of the ground during winters and possible infiltration of meltwater in the spring, although latent heat released in association with annual freezing and thawing of porewater may also play a role. The significant dryness of the Central Andes compared to other mountain environments, which has been exacerbated in recent years by the megadrought, also leads to comparatively less water available from snow melt to infiltrate the ground and promote permafrost degradation. Another possibility for lack of a clear warming trend in ground temperatures could be that temporary, localized surface temperature inversions are occurring, or have occurred in recent years, causing air temperatures at lower elevations in the dataset to be cooler than might otherwise be expected, and vice versa. Such inversions have been shown to lead to unique permafrost conditions in near-proximity dissimilar valleys in Yukon, Canada, with air temperatures at some high-altitude sites found to be significantly warmer than their adjacent valley bottoms (Noad and Bonnaventure, 2023).

https://doi.org/10.5194/egusphere-2024-2244
Preprint. Discussion started: 30 September 2024


At a more regional scale, the combined influence of the El Niño Southern Oscillation (ENSO) and Pacific Decadal Oscillation (PDO) on South American climate patterns (e.g., Mantua and Hare, 2002; Montecinos and Aceituno, 2003; Vuille et al., 2015; Garreaud et al., 2020; Yoshikawa et al., 2020) can exhibit temporary influence on the ground thermal regime across the study area. This would occur primarily through changes to spatial and temporal snowpack distribution and snow-albedo feedback, as well as through variations in water infiltration that can impact absorption of latent heat. Interactions of ENSO and IPO may have contributed to a decline in precipitation in the late 20$^{th}$ century (Schulz et al., 2012), potentially influencing historical ground temperatures. However, oceanic phenomena are presumed to have had little influence on the rainfall deficit associated with the megadrought that has persisted in Central Chile for the past two decades (Garreaud et al., 2020). Temperature and precipitation patterns directly related to the ENSO and PDO, and their potential impacts to the ground thermal regime, were not examined in this paper. However, some patterns are apparent for the Central Andes and may be applicable to the study area. This includes temporary cooling trends observed in shallow (2 m deep) ground temperatures simultaneously with deceleration of several rock glaciers at a site with permafrost in Central Chile (and located within the range of sites in this study) that coincided with lower MAATs during the same period (2010-2015). These cooling trends were postulated to be linked to the predominance of La Niña (cold and dry phase of the ENSO) and neutral ENSO conditions since 2009 (Vivero et al., 2021).

With a monitoring record that currently falls short of the ideal length to assess impacts of atmospheric warming on ground temperatures (i.e., 20 years or more), air temperature data collected in the study region may offer complimentary insights to the observations presented in this work. A summary of MAATs in mountainous regions in South America by (Hock et al., 2019), which is based on very limited monitoring data, illustrates lower warming rates or even slight cooling trends when compared to global studies. One meteorological station located at Site 3 (~5,000 m) demonstrates relatively stable air temperatures over 20 years of monitoring (1999-2021, Figure 15). This apparent stability and/or slight lowering of MAATs in South America suggests that the trajectory of ground temperatures in the Andes is also likely to be unique from other regions that show clear signs of warming. It is also worth noting that the unique topo-climatic attributes of the Andean cryosphere – specifically the combination of arid conditions, high solar radiation, lack of vegetative cover and organic matter, and less massive ice (except for rock glaciers) together with mountain topography – may expedite energy transfer processes and reduce latency of temperature change compared to other permafrost regions, both in mountains and the Arctic. Regardless of the specific mechanisms influencing ground temperature evolution in the Andes, the preceding discussions emphasize the importance of continued monitoring to establish robust connections with climate change. This effort must also consider local climate and geographic conditions, as well as relationships with oceanic phenomena.

https://doi.org/10.5194/egusphere-2024-2244
Preprint. Discussion started: 30 September 2024


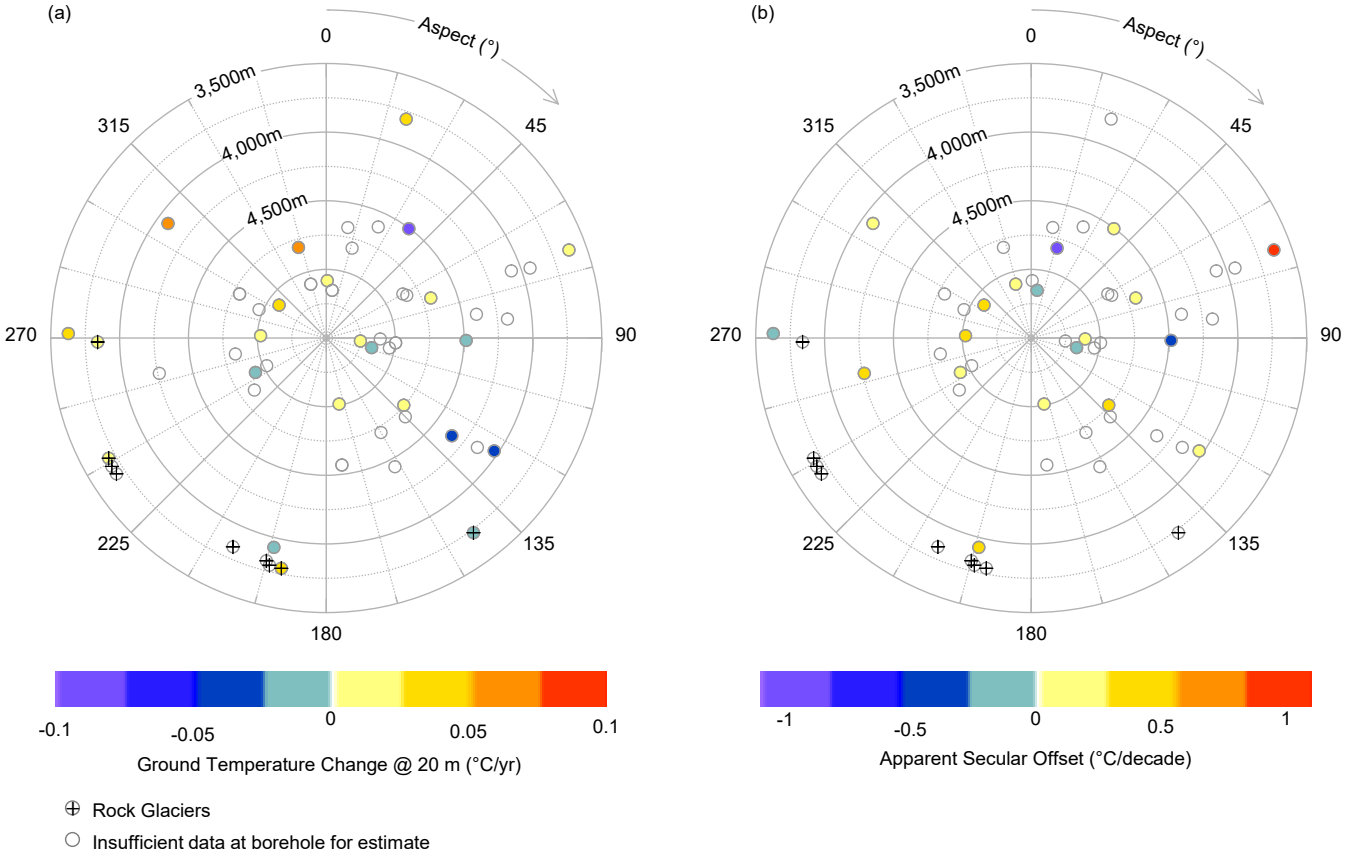


**Figure 14: Aspect-elevation diagrams showing variations in (a) ground temperature change and (b) apparent secular offset. Some estimates shown in (a) are from depths other than at 20m (i.e., at the maximum sensor depth for thermistor strings shorter than 20m, or depth adjusted to illustrate trends within cryotic zones).**

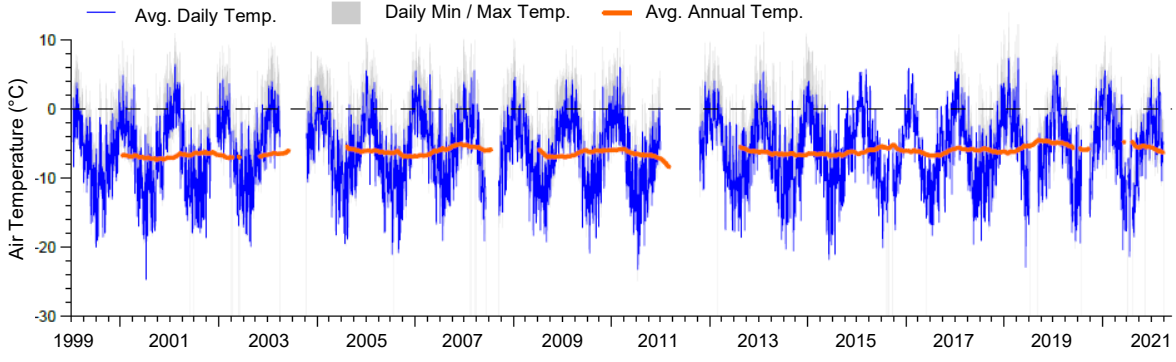


**Figure 15: Air temperature time series collected at Site 3 (El 4,927 m). Shows stability of temperature data over 20 years. Source: BGC Engineering Inc. (2021).**

https://doi.org/10.5194/egusphere-2024-2244
Preprint. Discussion started: 30 September 2024


### 5.3 Shared Characteristics with other Mountain Permafrost Regions

Although the topo-climatic conditions of the Andes are unique among permafrost zones, the ground temperature data compiled in this study illustrate some common characteristics with other mountain permafrost environments. Attributes of the dataset such as high spatial heterogeneity in ground temperatures, correlations with altitude and slope aspect, as well as distinct thermal characteristics of rock glaciers compared to other landforms, imply that analogous processes are shaping the current and changing ground thermal regime in the Central Andes.

Significant variations in ground temperature over short distances—shifting from cold to warm permafrost (< -2°C to 0°C) and/or non-cryotic ground within less than 5 km horizontally—emphasizes the strong microclimatic influence on the distribution of permafrost at catchment level over regional climate stressors. Together with nearby geophysical surveying efforts by Hilbich et al. (2022), this highlights the challenge of upscaling point information, such as boreholes and geophysical results, to larger catchments in the Andes (Mathys et al., 2022). The overall pattern of decreasing ground temperatures and depth to permafrost, and increasing permafrost thicknesses with increasing altitude, reflects an orographic influence of air temperatures across the dataset, which is an attribute common to mountainous regions.

The spatial pattern of ground temperatures with respect to slope aspect may reflect the asymmetry of incident solar radiation of the geographic region, resulting in a higher elevation of the zero-degree ground temperature isotherm on northeast facing slopes. These characteristics were previously assumed to exist for the Central Andes based on climate and mapping studies in the region (e.g., Saito et al., 2016), ground temperature characterizations in mountain permafrost elsewhere and general knowledge of mountain permafrost environments (e.g., Haeberli, 1973). However, until now they were not extensively illustrated with ground temperature data, and as discussed above, the findings of this study have created a new opportunity for permafrost researchers to validate their analyses of permafrost distribution in the region.

Also widely demonstrated for other mountain permafrost regions (e.g. Barsch, 1977), rock glaciers emerge as thermally unique permafrost features in the Andean dataset. This distinction of rock glaciers from other boreholes arises due to their characteristic coarse blocky morphology and resultant elevated porosity; attributes which enable substantial variations in air, water, and ground ice content. This variability is known to exert a significant influence on ground temperatures, both spatially and temporally, especially when rock glaciers contain substantial amounts of ice and near the phase change temperature (e.g., Haeberli et al., 2006). Ground temperatures within rock glaciers in the Andean dataset do not follow general altitudinal trends of other boreholes—instead, they consistently show lower temperatures than boreholes at similar elevations, likely due to the combination of reduced thermal conductivity and convective cooling in the blocky active layer and sustained presence of ground ice due to latent heat. Estimated depth to permafrost and permafrost thickness within rock glaciers also deviate from the broader elevation trends observed in the dataset, with a greater depth to permafrost consistent with rock glaciers marking the lower limit of permafrost in the dataset. Rock glaciers also exhibit the greatest and most variable depths to permafrost, and lowest estimated permafrost thickness within the dataset (i.e., > 7 m deep and approximately 2 m to 10 m thick in rock glaciers,

https://doi.org/10.5194/egusphere-2024-2244
Preprint. Discussion started: 30 September 2024


compared to typically < 4 m deep and > 40 m thick in other permafrost boreholes). The formation of a supra-permafrost talik at two locations (boreholes 6-1 and 6-4) reflects an advanced state of degradation observed in these landforms.

Finally, rock glaciers appear to mark the lowest altitudinal limit of permafrost in the Andean dataset – slightly below 3,700 m at Site 6, with the remainder of measurements in rock glaciers clustering near 0°C between elevations of 3,700 m and 3,800 m, and the majority of cryotic boreholes in the dataset not in rock glaciers occurring above 4,250 m. Although this estimate is roughly consistent with previously reported limits in the region (i.e., ranging between 2,900 m and 3,200 m, and occasionally reaching elevations of 3,700 m (Saito et al., 2016), caution is emphasized regarding the representativeness of the presented estimates due to sample coverage bias resulting from industry driven data collection needs rather than specific permafrost delineation objectives. The same caution applies in consideration of the asymmetry of the interpreted zero-degree ground temperature isotherm with respect to aspect for the full dataset. While rock glaciers occur on south-facing slopes and in areas that experience lower solar radiation, their absence on north facing slopes may partially be a consequence of sampling bias rather than influence of solar radiation.

## 6 Conclusion

This study represents the first regional compilation of in-situ ground temperature data collected from mountain permafrost regions of the Central Andes (27°S-34°S) at depths below seasonal influences. Compiled from 53 boreholes along a 650 km long north-south transect near the Chilean-Argentine border, the dataset contributes new insights that broaden the understanding of permafrost temperature dynamics in South America. The presented analyses demonstrate parallels with ground temperature characteristics of other mountain permafrost regions of the world, while also revealing aspects of the ground thermal regime unique to the Central Andes. Pronounced spatial variability in ground temperatures, correlations with altitude and slope aspect, and distinctive thermal attributes of rock glaciers relative to other landforms suggest that processes influencing the ground thermal regime in the Central Andes are analogous to other mountain permafrost environments. At the same time, the unique combination of topo-climatic and geomorphic attributes of the Andean cryosphere (including high aridity, solar radiation, lack of vegetation and organic matter, lower overall massive ice content combined with mountainous terrain) may enhance energy transfer with the ground compared to other permafrost regions. The length of monitoring in the dataset—less than ten years of consecutive measurements—currently does not allow for assessment of long-term trends in response to climate change. In addition, the region's susceptibility to oceanic phenomena such as ENSO and PDO, which occur on decadal timescales, implies that, in contrast to the northern hemisphere, it is likely that long-term ground temperature trends for the Central Andes may only be derived from very long time-series spanning several of these cycles. The observed temporal variability in the dataset thus reflects local topographic factors and short-term micro-climatic fluctuations unique to the catchment(s) monitored.

In addition to the insights gained from the analyses presented, this study creates an opportunity to validate and refine existing permafrost distribution models in the Andean region that were developed from indirect evidence of permafrost occurrence.

https://doi.org/10.5194/egusphere-2024-2244
Preprint. Discussion started: 30 September 2024


Integrating results of this study can improve the accuracy and reliability of these models, aligning them more closely with the well-calibrated models established for Europe and North America that benefit from extensive in-situ data. The presented dataset may also support upscaling efforts, which play a pivotal role in quantifying ground ice content in permafrost regions across broader spatial scales. Such endeavors are essential for informing predictive models, especially in the context of climate change, where accurate assessments of permafrost dynamics are crucial for effective water resource planning and decision-making. The integration of results from this compilation into such upscaling efforts thus holds promise for researchers to advance a more comprehensive understanding of interactions between permafrost and hydrology in the Andean region under ongoing global atmospheric warming.

Many of the data collection challenges outlined in this paper are common to mountain permafrost studies outside of the Andes. These include natural, logistical, and financial limitations, which occasionally led to interruptions or shortened monitoring records, or introduced artifacts into the collected data. In addition to these challenges, this study faced constraints stemming from industry needs and regulatory requirements, which dictated thermistor placement and influenced data collection and instrument maintenance schedules. Since monitoring objectives were required to align with needs of environmental impact assessments (EIAs), boreholes were established primarily to meet these needs, rather than for research purposes. Consequently, instrument positioning and data collection schedules were not optimized for permafrost characterization or long-term monitoring, as would be the case in a dedicated scientific research project.

It is possible that the current scarcity of in-situ data in the Central Andes is a reflection of compounding challenges of difficult terrain and significant sectorial constraints. In this sense, the present study represents a unique and exemplary collaboration between industry, academia, and bi-national regulators for the advancement of understanding of a key indicator of climate change in a region that is underrepresented in the Global Climate Observing System (GCOS) and permafrost literature. Through this collaboration, new insights into ground thermal characteristics of the Central Andes have been revealed, which were not previously demonstrated with ground-based data. This highlights the value and imperative for multi-stakeholder partnerships in advancing knowledge of thermal state of permafrost alongside other critical issues related to climate change.

## Competing interests

At least one of the (co-)authors is a member of the editorial board of The Cryosphere. This work was partially funded by BGC Engineering Inc and University of Fribourg as a graduate research project.

## Acknowledgements

The authors would like to acknowledge the team of engineers and scientists at BGC Ingenieria Ltda. in Chile and Argentina for the collection and processing of data presented in this paper. The support from BGC Engineering Inc. and their clients in providing the opportunity to compile and analyse this dataset is further acknowledged and appreciated.

https://doi.org/10.5194/egusphere-2024-2244
Preprint. Discussion started: 30 September 2024


## References

Abram, N., Gattuso, J.-P., Prakash, A., Cheng, L., Chidichimo, M. P., Crate, S. , Enomoto, H., Garschagen, M., Gruber, N., Harper, S., Holland, E., Kudela, R. M., Rice, J., Steffen, K., and von Schuckmann, K.: Framing and Context of the Report, in: IPCC Special Report on the Ocean and Cryosphere in a Changing Climate, edited by: Pörtner, H.-O., Roberts, D. C., Masson-Delmotte, V., Zhai, P., Tignor, M. , Poloczanska, E., Mintenbeck, K., Alegría, A., Nicolai, M., Okem, A., Petzold, J., Rama, B., and Weyer, N. M., Cambridge University Press, Cambridge, UK and New York, NY, USA, 78–129, 2019.

Andrés, N., Palacios, D., Úbeda, J., and Alcalá, J.: Ground Thermal Condition at Chachani Volcano, Southern Peru, Geografiska Annaler: Series A, Physical Geography, 93, 151–162, https://doi.org/https://doi.org/10.1111/j.1468-0459.2011.00424.x, 2011.

Arenson, L. U. and Jakob, M.: A New GIS based Mountain Permafrost Distribution Model, Proceedings, 63rd Canadian Geotechnical Conference & 6th Canadian Permafrost Conference, 2010.

Arenson, L. U., Harrington, J. S., Koenig, C. E. M., and Wainstein, P. A.: Mountain Permafrost Hydrology—A Practical Review Following Studies from the Andes, Geosciences (Basel), 12, https://doi.org/10.3390/geosciences12020048, 2022.

Atacama Ambiente: Estudio de caracterización de temperaturas subsuperficiales mediante cintas termistoras, proyecto minero Salares Norte. Santiago: En: Estudio de impacto ambiental Salares Norte. Goldfields. Anexo 3.2.11-11. Soluciones de Gestión Ambiental, SGA., 2017.

Barsch, D.: Nature and importance of mass-wasting by rock glaciers in alpine permafrost environments, Earth Surface Processes, 2, 231–245, https://doi.org/https://doi.org/10.1002/esp.3290020213, 1977.

Biskaborn, B. K., Lanckman, J.-P., Lantuit, H., Elger, K., Streletskiy, D. A., Cable, W. L., and Romanovsky, V. E.: The new database of the Global Terrestrial Network for Permafrost (GTN-P), Earth Syst Sci Data, 7, 245–259, https://doi.org/10.5194/essd-7-245-2015, 2015.

Biskaborn, B. K., Smith, S. L., Noetzli, J., Matthes, H., Vieira, G., Streletskiy, D. A., Schoeneich, P., Romanovsky, V. E., Lewkowicz, A. G., Abramov, A., Allard, M., Boike, J., Cable, W. L., Christiansen, H. H., Delaloye, R., Diekmann, B., Drozdov, D., Etzelmüller, B., Grosse, G., Guglielmin, M., Ingeman-Nielsen, T., Isaksen, K., Ishikawa, M., Johansson, M., Johannsson, H., Joo, A., Kaverin, D., Kholodov, A., Konstantinov, P., Kröger, T., Lambiel, C., Lanckman, J.-P., Luo, D., Malkova, G., Meiklejohn, I., Moskalenko, N., Oliva, M., Phillips, M., Ramos, M., Sannel, A. B. K., Sergeev, D., Seybold, C., Skryabin, P., Vasiliev, A., Wu, Q., Yoshikawa, K., Zheleznyak, M., and Lantuit, H.: Permafrost is warming at a global scale, Nat Commun, 10, 264, https://doi.org/10.1038/s41467-018-08240-4, 2019.

Brown, J., Hinkel, K., and Nelson, F.: The Circumpolar Active Layer Monitoring (CALM) program, Polar Geography, 24, 166–258, https://doi.org/10.1080/10889370009377698, 2000.

https://doi.org/10.5194/egusphere-2024-2244
Preprint. Discussion started: 30 September 2024


Bruniard, E. D.: La Diagonal Árida Argentina: un Límite Climático Real, Revista Geográfica, 5–20, 1982.

Carrasco, J., Casassa, G., and Quintana, J.: Changes of the 0°C isotherm and the equilibrium line altitude in central Chile during the last quarter of the 20th century / Changements de l'isotherme 0°C et de la ligne d'équilibre des neiges dans le Chili central durant le dernier quart du 20ème siècle, Hydrological Sciences Journal/Journal des Sciences Hydrologiques, 50, 948, https://doi.org/10.1623/hysj.2005.50.6.933, 2005.

Catalano, L. R.: Contribución al Conocimiento de los Fenómenos Geofícos Atmosféricos (en base a observaciones efectuadas en la Puna de Atacama, territorio nacional de Los Andes), Ministerio de Agricultura. Dirección General de Minas, Geología e Hidrología, Buenos Aires, 1926.

Christiansen, H. H., Etzelmüller, B., Isaksen, K., Juliussen, H., Farbrot, H., Humlum, O., Johansson, M., Ingeman-Nielsen, T., Kristensen, L., Hjort, J., Holmlund, P., Sannel, A. B. K., Sigsgaard, C., Åkerman, H. J., Foged, N., Blikra, L. H., Pernosky, M. A., and Ødegård, R. S.: The thermal state of permafrost in the nordic area during the international polar year 2007–2009, Permafr Periglac Process, 21, 156–181, https://doi.org/https://doi.org/10.1002/ppp.687, 2010.

Corte A: Contribución a Ia Morfología Periglacial de Ia Alta Cordillera con Especial Mención deI Aspecto Criopedológico, 54 pp., 1953.

Derksen, C., Burgess, D., Duguay, C., Howell, S., Mudryk, L., Smith, S., Thackeray, C., and Kirchmeier-Young, M.: Changes in snow, ice, and permafrost across Canada, in: Canada's Changing Climate Report, edited by: Bush, E. and Lemmen, D. S., Government of Canada, Ottawa, Ontario, 194–260, 2019.

Dirección General de Aguas (DGA): Dinámica de glaciares rocosos en el Chile semiárido. Technical report, Santiago de Chile, 2010.

Dirección General de Aguas (DGA): Plan de Monitoreo Nacional de Permafrost, Santiago de Chile, 2019.

Dobiński, W.: Permafrost active layer, Earth Sci Rev, 208, 103301, https://doi.org/https://doi.org/10.1016/j.earscirev.2020.103301, 2020.

Etzelmüller, B., Guglielmin, M., Hauck, C., Hilbich, C., Hoelzle, M., Isaksen, K., Noetzli, J., Oliva, M., and Ramos, M.: Twenty years of European mountain permafrost dynamics—the PACE legacy, Environmental Research Letters, 15, 104070, https://doi.org/10.1088/1748-9326/abae9d, 2020.

van Everdingen, R. O.: Multi-Language Glossary of Permafrost and Related Ground ice Terms (Revised 2005); International Permafrost Association: Ottawa, ON, Canada, 1998.

Falvey, M. and Garreaud, R. D.: Regional cooling in a warming world: Recent temperature trends in the southeast Pacific and along the west coast of subtropical South America (1979–2006), Journal of Geophysical Research: Atmospheres, 114, https://doi.org/https://doi.org/10.1029/2008JD010519, 2009.

Garreaud, R.: The Andes Climate and Weather, Adv. Geosci, 22, 3–11, https://doi.org/10.5194/adgeo-22-3-2009, 2009.

Garreaud, R., Boisier, J. P., Rondanelli, R., Montecinos, A., Sepúlveda, H., and Veloso, D.: The Central Chile Mega Drought (2010-2018): A Climate dynamics perspective, International Journal of Climatology, 40, https://doi.org/10.1002/joc.6219, 2020.

https://doi.org/10.5194/egusphere-2024-2244
Preprint. Discussion started: 30 September 2024


Gruber, S. and Haeberli, W.: Permafrost in steep bedrock slopes and its temperature-related destabilization following climate change, J Geophys Res Earth Surf, 112, https://doi.org/https://doi.org/10.1029/2006JF000547, 2007.

Haberkorn, A., Kenner, R., Noetzli, J., and Phillips, M.: Changes in Ground Temperature and Dynamics in Mountain Permafrost in the Swiss Alps, Front Earth Sci (Lausanne), 9, 626686, https://doi.org/10.3389/feart.2021.626686, 2021.

Haeberli, W.: Die Basis-Temperatur der winterlichen Schneedecke als moglicher indikator fur die Verbreitung von permafrost in den Alpen, Zeitschrift für Gletscherkunde Und Glazialgeologie, 9, 221–227, 1973.

Haeberli, W., Hallet, B., Arenson, L., Elconin, R., Humlum, O., Kääb, A., Kaufmann, V., Ladanyi, B., Matsuoka, N., Springman, S., and Mühll, D. V.: Permafrost creep and rock glacier dynamics, Permafr Periglac Process, 17, 189–214, https://doi.org/https://doi.org/10.1002/ppp.561, 2006.

Halla, C., Blöthe, J. H., Tapia Baldis, C., Trombotto Liaudat, D., Hilbich, C., Hauck, C., and Schrott, L.: Ice content and interannual water storage changes of an active rock glacier in the dry Andes of Argentina, Cryosphere, 15, 1187–1213, https://doi.org/10.5194/tc-15-1187-2021, 2021.

Hauck, C., Böttcher, M., and Maurer, H.: A new model for estimating subsurface ice content based on combined electrical and seismic data sets, Cryosphere, 5, https://doi.org/10.5194/tc-5-453-2011, 2011.

Hilbich, C., Hauck, C., Mollaret, C., Wainstein, P., and Arenson, L. U.: Towards accurate quantification of ice content in permafrost of the Central Andes – Part 1: Geophysics-based estimates from three different regions, Cryosphere, 16, 1845–1872, https://doi.org/10.5194/tc-16-1845-2022, 2022.

Hock, R., Rasul, G., Adler, C., Cáceres, B., Gruber, S., Hirabayashi, Y., Jackson, M., Kääb, A., Kang, S., Kutuzov, S., Milner, Al., Molau, U., Morin, S., Orlove, B., and and H. Steltzer: High Mountain Areas, in: IPCC Special Report on the Ocean and Cryosphere in a Changing Climate, edited by: Pörtner, H.-O., Roberts, D. C., Masson-Delmotte, V., Zhai, P., M., T., Poloczanska, E., Mintenbeck, K., Alegría, A., Nicolai, M., Okem, A., Petzold, J., Rama, B., and Weyer, N. M., Cambridge University Press, 131–202, https://doi.org/10.1017/9781009157964.003, 2019.

Isaksen, K., Sollid, J. L., Holmlund, P., and Harris, C.: Recent warming of mountain permafrost in Svalbard and Scandinavia, J Geophys Res Earth Surf, 112, https://doi.org/https://doi.org/10.1029/2006JF000522, 2007.

Jacques-Coper, M. and Garreaud, R. D.: Characterization of the 1970s climate shift in South America, International Journal of Climatology, 35, 2164–2179, https://doi.org/https://doi.org/10.1002/joc.4120, 2015.

Jones, D. B., Harrison, S., Anderson, K., and Whalley, W. B.: Rock glaciers and mountain hydrology: A review, Earth Sci Rev, 193, 66–90, https://doi.org/https://doi.org/10.1016/j.earscirev.2019.04.001, 2019.

Kokelj, S. V, Lantz, T. C., Tunnicliffe, J., Segal, R., and Lacelle, D.: Climate-driven thaw of permafrost preserved glacial landscapes, northwestern Canada, Geology, 45, 371–374, https://doi.org/10.1130/G38626.1, 2017.

Kottek, M., Grieser, J., Beck, C., Rudolf, B., and Rubel, F.: World Map of the Köppen-Geiger Climate Classification Updated, Meteorologische Zeitschrift, 15, 259–263, https://doi.org/10.1127/0941-2948/2006/0130, 2006.

Koven, C. D., Lawrence, D. M., and Riley, W. J.: Permafrost carbon−climate feedback is sensitive to deep soil carbon decomposability but not deep soil nitrogen dynamics, Proceedings of the National Academy of Sciences, 112, 3752–3757, https://doi.org/10.1073/pnas.1415123112, 2015.

Krautblatter, M., Verleysdonk, S., Flores Orozco, A., and Kemna, A.: Temperature-calibrated imaging of seasonal changes in permafrost rock walls by quantitative electrical resistivity tomography (Zugspitze, German/Austrian Alps), J Geophys Res, 115, https://doi.org/10.1029/2008JF001209, 2010.

Lachenbruch, A. H. and Marshall, B. V.: Changing Climate: Geothermal Evidence from Permafrost in the Alaskan Arctic, Science (1979), 234, 689–696, 1986.

Luethi, R., Phillips, M., and Lehning, M.: Estimating Non-Conductive Heat Flow Leading to Intra-Permafrost Talik Formation at the Ritigraben Rock Glacier (Western Swiss Alps), Permafr Periglac Process, 28, 183–194, https://doi.org/https://doi.org/10.1002/ppp.1911, 2017.

Mantua, N. and Hare, S.: The Pacific Decadal Oscillation, J Oceanogr, 58, 35–44, https://doi.org/10.1023/A:1015820616384, 2002.

Masiokas, M., Christie, D., Quesne, C., Pitte, P., Ruiz, L., Villalba, R., Luckman, B., Berthier, E., Nussbaumer, S., Gonzalez Reyes, A., Mcphee, J., and Barcaza, G.: Reconstructing the annual mass balance of the Echaurren Norte glacier (Central Andes, 33.5° S) using local and regional hydroclimatic data, Cryosphere, 10, 927–940, https://doi.org/10.5194/tc-10-927-2016, 2016.

Masiokas, M. H., Rabatel, A., Rivera, A., Ruiz, L., Pitte, P., Ceballos, J. L., Barcaza, G., Soruco, A., Bown, F., Berthier, E., Dussaillant, I., and MacDonell, S.: A Review of the Current State and Recent Changes of the Andean Cryosphere, Front Earth Sci (Lausanne), 8, https://doi.org/10.3389/feart.2020.00099, 2020.

Mathys, T., Hilbich, C., Arenson, L. U., Wainstein, P. A., and Hauck, C.: Towards accurate quantification of ice content in permafrost of the Central Andes – Part 2: An upscaling strategy of geophysical measurements to the catchment scale at two study sites, Cryosphere, 16, 2595–2615, https://doi.org/10.5194/tc-16-2595-2022, 2022.

Mena, G., Yoshikawa, K., Schorghofer, N., Pasten, C., Ochoa-Cornejo, F., Yoshii, Y., Doi, M., Miyata, T., Takahashi, H., Casassa, G., and Sone, T.: Freeze–thaw cycles and snow impact at arid permafrost region in Chajnantor Volcano, Atacama, northern Chile, Arct Antarct Alp Res, 53, 60–66, https://doi.org/10.1080/15230430.2021.1878739, 2021.

Miner, K. R., Malina, E., and Bartsch, A.: Permafrost carbon emissions in a changing Arctic, Nat Rev Earth Environ, 55–67, https://doi.org/10.1038/s43017-021-00230-3, 2022.

Mollaret, C., Wagner, F., Hilbich, C., Scapozza, C., and Hauck, C.: Petrophysical Joint Inversion Applied to Alpine Permafrost Field Sites to Image Subsurface Ice, Water, Air, and Rock Contents, Front Earth Sci (Lausanne), 8, 85, https://doi.org/10.3389/feart.2020.00085, 2020.

Monnier, S. and Kinnard, C.: Internal structure and composition of a rock glacier in the Andes (upper Choapa valley, Chile) using borehole information and ground-penetrating radar, Ann Glaciol, 54, 61–72, https://doi.org/10.3189/2013AoG64A107, 2013.

https://doi.org/10.5194/egusphere-2024-2244
Preprint. Discussion started: 30 September 2024


Montana, J., Morales, C., Nicora, M. G., Ardila, J., Schurch, R., and Aranguren, D.: Lightning Activity Over Chilean Territory, Journal of Geophysical Research: Atmospheres, 126, e2021JD034580, https://doi.org/https://doi.org/10.1029/2021JD034580, 2021.

Montecinos, A. and Aceituno, P.: Seasonality of the ENSO-Related Rainfall Variability in Central Chile and Associated Circulation Anomalies, Journal of Climate - J CLIMATE, 16, 281–296, https://doi.org/10.1175/1520-0442(2003)016<0281:SOTERR>2.0.CO;2, 2003.

Nagy, B., Ignéczi, Á., Kovács, J., Szalai, Z., and Mari, L.: Shallow ground temperature measurements on the highest volcano on Earth, Mt. Ojos del Salado, Arid Andes, Chile, Permafr Periglac Process, 30, 3–18, https://doi.org/https://doi.org/10.1002/ppp.1989, 2019.

Noad, N. C. and Bonnaventure, P. P.: Examining the influence of microclimate conditions on the breakup of surface-based temperature inversions in two proximal but dissimilar Yukon valleys, Canadian Geographies / Géographies canadiennes, n/a, https://doi.org/https://doi.org/10.1111/cag.12886, 2023.

Noetzli, J., Arenson, L. U., Bast, A., Beutel, J., Delaloye, R., Farinotti, D., Gruber, S., Gubler, H., Haeberli, W., Hasler, A., Hauck, C., Hiller, M., Hoelzle, M., Lambiel, C., Pellet, C., Springman, S. M., Vonder Muehll, D., and Phillips, M.: Best Practice for Measuring Permafrost Temperature in Boreholes Based on the Experience in the Swiss Alps, Front Earth Sci (Lausanne), 9, https://doi.org/10.3389/feart.2021.607875, 2021.

Nyland, K. E., Shiklomanov, N. I., Streletskiy, D. A., Nelson, F. E., Klene, A. E., and Kholodov, A. L.: Long-term Circumpolar Active Layer Monitoring (CALM) program observations in Northern Alaskan tundra, Polar Geography, 44, 167–185, https://doi.org/10.1080/1088937X.2021.1988000, 2021.

PERMOS: Permafrost in Switzerland 2014/2015 to 2017/2018, in: Glaciological Report Permafrost No. 16–19 of the Cryospheric Commission of the Swiss Academy of Sciences, vol. 16–19, edited by: Noetzli, J. , Pellet, C., and and Staub, B., 104, 2019.

PERMOS: Swiss Permafrost Bulletin 2022, edited by: Noetzli, J. and Pellet, C., 23 pp., 2023.

Romanovsky, V., Smith, S., and Christiansen, H.: Permafrost Thermal State in the Polar Northern Hemisphere during the International Polar Year 2007–2009: a Synthesis, Permafr Periglac Process, 21, 106–116, https://doi.org/10.1002/ppp.689, 2010a.

Romanovsky, V., Drozdov, D., Oberman, N., Malkova, G., Kholodov, A., Marchenko, S., Moskalenko, N., Sergeev, D., Ukraintseva, N., Abramov, A., Gilichinsky, D., and Alexander, V.: Thermal State of Permafrost in Russia, Permafr Periglac Process, 21, 136–155, https://doi.org/10.1002/ppp.683, 2010b.

Romanovsky, V., Isaksen, K., D, D., Anisimov, O., A, I., Leibman, M., AD, M., Shiklomanov, N., S, S., and D, W.: Changing permafrost and its impacts. In: Snow, Water, Ice and Permafrost in the Arctic (SWIPA) 2017, 65–102, 2017.

Ruiz, L. and Trombotto, D.: Mountain permafrost distribution in the Andes of Chubut (Argentina) based on a statistical model, Proceedings, Tenth International Conference on Permafrost (TICOP) Salekhard, Russia, 365–370, 2012.

https://doi.org/10.5194/egusphere-2024-2244
Preprint. Discussion started: 30 September 2024


Saito, K., Trombotto Liaudat, D., Yoshikawa, K., Mori, J., Sone, T., Marchenko, S., Romanovsky, V., Walsh, J., Hendricks, A., and Bottegal, E.: Late Quaternary Permafrost Distributions Downscaled for South America: Examinations of GCM-based Maps with Observations, Permafr Periglac Process, 27, 43–55, https://doi.org/https://doi.org/10.1002/ppp.1863, 2016.

Schaefer, K., Lantuit, H., Romanovsky, V., Schuur, E., and Witt, R.: The impact of the permafrost carbon feedback on global climate, Environmental Research Letters, 9, 85003, https://doi.org/10.1088/1748-9326/9/8/085003, 2014.

Schulz, N., Boisier, J. P., and Aceituno, P.: Climate change along the arid coast of northern Chile, International Journal of Climatology, 32, 1803–1814, https://doi.org/https://doi.org/10.1002/joc.2395, 2012.

Schuur, E., McGuire, A. D., Schädel, C., Grosse, G., Harden, J., Hayes, D. J., Hugelius, G., Koven, C., Kuhry, P., Lawrence, D., Natali, S., Olefeldt, D., Romanovsky, V., Schaefer, K., Turetsky, M., Treat, C., and Vonk, J.: Climate change and the permafrost carbon feedback, Nature, 2015, 171–179, https://doi.org/10.1038/nature14338, 2015.

Schuur, E. A. G., Vogel, J. G., Crummer, K. G., Lee, H., Sickman, J. O., and Osterkamp, T. E.: The effect of permafrost thaw on old carbon release and net carbon exchange from tundra, Nature, 459, 556–559, https://doi.org/10.1038/nature08031, 2009.

Schuur, E. A. G., Abbott, B. W., Commane, R., Ernakovich, J., Euskirchen, E., Hugelius, G., Grosse, G., Jones, M., Koven, C., Leshyk, V., Lawrence, D., Loranty, M. M., Mauritz, M., Olefeldt, D., Natali, S., Rodenhizer, H., Salmon, V., Schädel, C., Strauss, J., Treat, C., and Turetsky, M.: Permafrost and Climate Change: Carbon Cycle Feedbacks From the Warming Arctic, Annu Rev Environ Resour, 47, 343–371, https://doi.org/10.1146/annurev-environ-012220-011847, 2022.

Smith, S., O'Neill, H. B., Isaksen, K., Noetzli, J., and Romanovsky, V.: The changing thermal state of permafrost, Nat Rev Earth Environ, 3, 10–23, https://doi.org/10.1038/s43017-021-00240-1, 2022.

Streletskiy, D., Biskaborn, B., Smith, S., Noetzli, J., Vieira, G., and Schoeneich, P.: Strategy and Implementation Plan 2016-2020 for the Global Terrestrial Network for Permafrost (GTN-P)., April 2017.

Trombotto, D. and Borzotta, E.: Indicators of present global warming through changes in active layer-thickness, estimation of thermal diffusivity and geomorphological observations in the Morenas Coloradas rockglacier, Central Andes of Mendoza, Argentina, Cold Reg Sci Technol, 55, 321–330, https://doi.org/https://doi.org/10.1016/j.coldregions.2008.08.009, 2009.

Trombotto, D., Buk, E., and Hernández, J.: Monitoring of Mountain Permafrost in the Central Andes, Argentina, Permafr Periglac Process, 8, 123–129, 1997.

Vivero, S., Bodin, X., Farías-Barahona, D., MacDonell, S., Schaffer, N., Robson, B. A., and Lambiel, C.: Combination of Aerial, Satellite, and UAV Photogrammetry for Quantifying Rock Glacier Kinematics in the Dry Andes of Chile (30°S) Since the 1950s, Frontiers in Remote Sensing, 2, https://doi.org/10.3389/frsen.2021.784015, 2021.

Vuille, M., Bradley, R., Werner, M., and Keimig, F.: 20th Century Climate Change in the Tropical Andes: Observations and Model Results, Climatic Change, v.59, 75-99 (2003), 59, https://doi.org/10.1023/A:1024406427519, 2003.

Vuille, M., Franquist, E., Garreaud, R., Lavado, W., and Cáceres, B.: Impact of the global warming hiatus on Andean temperature: Global warming hiatus in the Andes, Journal of Geophysical Research: Atmospheres, 120, https://doi.org/10.1002/2015JD023126, 2015.

https://doi.org/10.5194/egusphere-2024-2244
Preprint. Discussion started: 30 September 2024


Wicky, J. and Hauck, C.: Air Convection in the Active Layer of Rock Glaciers, Front Earth Sci (Lausanne), 8, https://doi.org/10.3389/feart.2020.00335, 2020.

World Meteorological Organization (WMO): The Global Observing System for Climate: Implementation Needs. WMO Publication No. GCOS – 200. https://library.wmo.int/doc_num.php?explnum_id=3417, 2016.

Yoshikawa, K., Úbeda, J., Masías, P., Pari, W., Apaza, F., Vasquez, P., Ccallata, B., Concha, R., Luna, G., Iparraguirre, J., Ramos, I., la Cruz, G., Cruz, R., Pellitero, R., and Bonshoms, M.: Current thermal state of permafrost in the southern Peruvian Andes and potential impact from El Niño–Southern Oscillation (ENSO), Permafr Periglac Process, 31, 598–609, https://doi.org/https://doi.org/10.1002/ppp.2064, 2020.

Zhang, T.: Influence of the seasonal snow cover on the ground thermal regime: An overview, Reviews of Geophysics, 43, https://doi.org/https://doi.org/10.1029/2004RG000157, 2005.